FACULTY OF PHARMACEUTICAL SCIENCES

Histone post-translational modifications as potential biomarkers for T-ALL treatment and their role in personalized medicine

Osman Satilmis

A Master dissertation for the study program Master in Drug Development

Academic year: 2021 – 2022

GHENT UNIVERSITY

SUMMARY

T-cell acute lymphoblastic leukemia (T-ALL) is a hematological cancer with one of the highest frequencies of altered epigenetic regulations among other tumors, suggesting that epigenetic aberrations play a crucial role in T-ALL development. Epigenetic modifications, including histone post-translational modifications (hPTMs) and DNA methylation, cause alterations in gene expression without changing the DNA sequence itself and thereby could influence the cell phenotype. Current treatment protocols often result in dose-dependent toxicity, relapse and poor treatment response. Given these issues, better treatment stratification is needed, whereby pharmacoepigenetics, which studies the epigenetic basis for individual variation in drugs response, could be helpful.

Six different epidrugs, namely three DNA methyltransferase inhibitors (DNMTis) and three histone deacetylase inhibitors (HDACis), which can restore epigenetic aberrations, were tested to link dose-response of 21 different T-ALL cell lines to their baseline hPTM levels. First, the 21 cell lines were treated with a dilution series of the six drugs, namely azacytidine (AZA), decitabine (DAC), GSK3685032 (GSK), panobinostat (PAN), vorinostat (VOR) and romidepsin (ROM) and cell viability was measured using Cell Titer Glo. Then, survival curves were plotted and IC50 and AUC values for each cell line were determined using GraphPad Prism. Finally, the IC50 and AUC values were linked to the baseline hPTM levels of the cell lines using Spearman correlation and PCA.

Successfully, AZA, VOR, ROM and PAN reduced the viability of most cell lines to 0%. However, DAC and GSK demonstrated low efficacy, since a minority of cell lines reached 0% viability at the highest concentration. Furthermore, positive correlations were found between methylation of histones and IC50- and AUC values for AZA and DAC. These correlations indicate that a high histone methylation level is linked with resistance to these DNMTis. Unfortunately, no significant correlations were found for GSK. As for the HDACis, IC50 values of ROM were positive correlated with histone acetylation, which indicates that hyperacetylation is linked to resistance of the cell lines to ROM. As for PAN and VOR, no significant correlations were found between hPTMs and IC50 or AUC values.

SAMENVATTING

T-cel acute lymfoblastische leukemie (T-ALL) is een hematologische kanker met een van de hoogste frequenties van afwijkende epigenetische regulaties onder andere tumoren, wat suggereert dat epigenetische afwijkingen een cruciale rol spelen in de ontwikkeling van T-ALL. Epigenetische modificaties, waaronder histon post-translationele modificaties (hPTMs) en DNA methylering, veroorzaken veranderingen in genexpressie zonder de DNA-sequentie zelf te veranderen en kunnen daarbij mogelijks het fenotype van de cel beïnvloeden. De huidige behandelingsprotocollen resulteren vaak in dosisafhankelijke toxiciteit, terugval en slechte respons op de behandeling. Gezien deze problemen is er een betere stratificatie van de behandeling nodig, waarbij farmaco-epigenetica, die de epigenetische basis bestudeert voor individuele variatie in de respons op geneesmiddelen, van nut kan zijn.

Zes verschillende epidrugs, namelijk drie DNA methyltransferase inhibitoren (DNMTis) en drie histone deacetylase inhibitoren (HDACis), die de epigenetische afwijkingen kunnen herstellen, worden getest om de dosis-respons van 21 verschillende T-ALL cellijnen te koppelen aan hun baseline hPTM niveaus. Eerst werden de 21 cellijnen behandeld met verdunningsreeksen van de zes geneesmiddelen, namelijk azacytidine (AZA), decitabine (DAC), GSK3685032 (GSK), panoninostat (PAN), vorinostat (VOR) en romidepsin (ROM) en de levensvatbaarheid van de cellen werd gemeten met behulp van Cell Titer Glo. Vervolgens werden de survival curves uitgezet, waarna de IC50- en AUC-waarden voor elke cellijn werden bepaald met GraphPad Prism. Tenslotte werden de IC50- en AUC-waarden gekoppeld aan de hPTM-niveaus met behulp van Spearman-correlatie en PCA.

Met succes verminderden AZA, VOR, ROM en PAN de levensvatbaarheid van de meeste cellijnen tot 0%. DAC en GSK toonden echter een geringe werkzaamheid, aangezien een minderheid van de cellijnen een levensvatbaarheid van 0% bereikte bij de hoogste concentratie. Bovendien werden positieve correlaties gevonden tussen methylering van histon-eiwitten en IC50- en AUC-waarden voor AZA en DAC.

Deze correlaties wijzen erop dat een hoog histon-methyleringsniveau samenhangt met resistentie tegen deze DNMTis. Helaas werden voor GSK geen significante correlaties gevonden. Wat de HDACis betreft, waren de IC50-waarden van ROM positief gecorreleerd met histonacetylering, wat erop wijst dat hyperacetylering verband houdt met resistentie van de cellijnen tegen ROM. Wat betreft voor PAN en VOR, werden er geen significante correlaties gevonden tussen hPTM's en IC50- of AUC-waarden.

DANKWOORD

De aanwezigen tijdens deze intensieve, maar toch enorm leerrijke periode wil ik één voor één bedanken:

Eerst en vooral wil ik Laura Corveleyn bedanken voor de fantastische begeleiding, waarbij ze een bron van inspiratie en motivatie was.

Maarten Dhaenens, voor het warm- en enthousiast verwelkomen.

Béatrice Lintermans, voor het kweken van de cellen en haar positiviteit.

Lien Provez, voor het geloven in me en beantwoorden van de knagende vragen.

De onderzoekers uit het MRB2 gebouw, voor de aangename sfeer.

De mede thesisstudenten, Robin Pagliuca, Rachana Kandel en Mary Ampofo voor hun morele steun en lachrijke momenten.

Mijn ouders en broer, voor het telkens bieden van een luisterend oor en het tonen van geduld.

Een algemene dank aan Universiteit Gent om mij de oppurtiniteit te geven om kennis op te doen en onderzoek te verrichten.

LIST WITH ABBREVIATIONS

AUC	Area under the curve
AZA	Azacytidine
BETi	Bromo and extra terminal domain inhibitor
CID	Collision induced dissociation
circRNA	circular RNA
CpG	Cytosine-phosphate-guanine
DAC	Decitabine
DC	Direct current
DDA	Data dependent acquisition
DIA	Data independent acquisition
DMETs	drug metabolizing enzymes and transporters
DNA	Deoxyribonucleic Acid
DNMT	DNA Methyl Transferase
DNMTi	DNA methyltransferase inhibitor
EM	Electron Multiplier
ESI	Electron Spray Ionization
HAT	Histone acetyltransferase
HDAC	Histone deacetylase
HDACi	histone deacetylase inhibitor
HDMi	histone demethylase inhibitor
HMTi	histone methyltransferase inhibitor
hPTM	histone post translational modification
K	Lysine

KDM6B	lysine demethylases 6B
LC-MS/MS	Liquid chromatography coupled to tandem mass spectrometry
lncRNA	long non-coding RNA
MCP	Microchannel plate
MDS	myelodysplastic syndrome
miRNA	micro RNA
MRS	Minimal residual disease
ncRNA	non-coding RNA
PCA	Principal Component Analysis
PMS	peptide mass fingerprint
PRC	Polycomb Repressive Complex
PRM	parallel monitoring
PXR	Pregnane X receptor
Q-TOF	quadrupole time-of-flight
R	Arginine
RF	Radio frequency
RISC	RNA-induced silencing complex
RNA	Ribonucleic Acid
RP-HPLC	reversed phase high performance liquid chromatography
S	Serine
SAM	S-adenosylmethionine
SRM	selected reaction monitoring
T	Threonine
T-ALL	T-cell acute lymphoblastic leukemia

TSG	Tumor suppressor genes
XIC	extracted ion chromatogram
Y	Tyrosine

1. INTRODUCTION

1.1. EPIGENETICS

1.1.1. General introduction

Nearly all our cells contain DNA, which is made up of four different nucleotides, i.e. adenine, guanine, thymine and cytosine. The order of these nucleotides, also called DNA sequence, contains information for specific heritable traits. This sequence is largely the same among the human population, although there are important differences. The variation in DNA sequence is caused by mutations, insertions, deletions and translocations, which leads to inter-individual variability. Furthermore, DNA is packaged as compact chromosomes inside the cell nucleus. This packaging is possible due to the presence of histones, which are positively charged proteins. DNA is negatively charged, which, in effects, means there is a strong histone-DNA interaction (1–3).

Modifying histones or DNA influences the chromosome structure, which can be euchromatic as well as heterochromatic. Heterochromatin refers to a highly condensed and thus less accessible chromosome, which in turn leads to transcription inactivity. Contrarily, euchromatin is loosely packed, more accessible and easily transcribed. In addition to DNA and histone modifications, posttranscriptional regulation of RNA can also influence gene expression. These modifications, causing alterations in gene expression without changing the DNA sequence itself, are studied by epigenetics. According to a Cold Spring Harbor meeting in 2008, epigenetics is defined as *"stable heritable phenotype resulting from changes in a chromosome without alterations in the DNA sequence".* The three main epigenetic modifications, namely DNA methylation, histone modifications and non-coding RNAs are shown in **figure 1.1** and briefly described in the following sections (2–6).

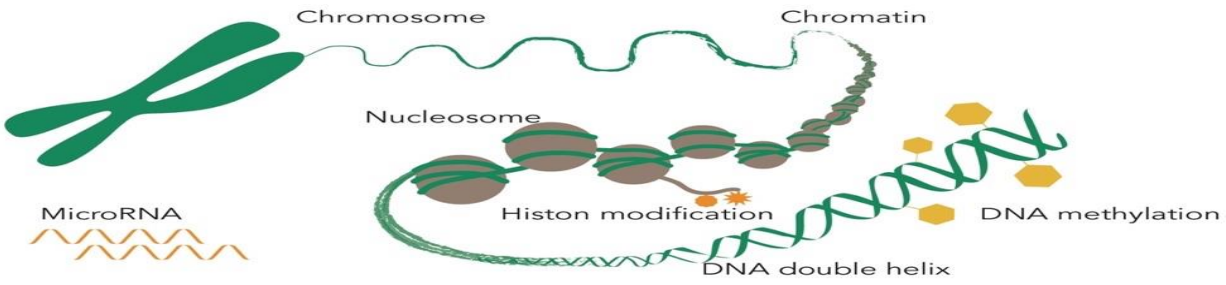

Figure 1.1: The DNA double helix wrapped around histones forming a nucleosome, which further compacts into chromatin and finally a chromosome. The three main epigenetic influences are represented; namely DNA methylation, histone modifications and small non-coding microRNA (7).

1.1.2. DNA methylation

DNA methylation is an epigenetic mechanism where a cytosine followed by a guanine (CpG site) is methylated at the C5 position, forming 5-methylcytosine (5mC). This reaction is catalyzed by DNA methyltransferases (DNMT's) using the methyl donor S-adenosylmethionine (SAM). It regulates gene expression by recruiting proteins or by blocking the binding of transcription factors to DNA. For instance, methylated DNA along with DNMT's recruit enzymes, such as histone deacetylases, providing modification of the histone N-tails by removing acetyl groups. This specific epigenetic crosstalk between DNA methylation and histone modification causes gene repression (8,9).

1.1.3. Non-coding RNA's

The largest fraction of RNA is non-coding RNA (ncRNA), which is not translated into proteins. However, ncRNA such as long non-coding RNAs (lncRNAs) and small micro-RNAs (miRNAs) carry out important functions in terms of gene expression. In the RNA-induced-silencing-complex (RISC), miRNAs bind Argonaute proteins, which leads to binding and cleaving of the complementary mRNA. As a result, translation of the complementary strands are hampered. LncRNAs are by definition ncRNAs consisting of more than 200 nucleotides, which also exert complementary mRNA binding and interaction with miRNAs. Further, this indicates that LncRNAs regulate gene expression (10,11).

1.1.4. Histones

1.1.4.1. Variants

As mentioned before, histones are essential to organize DNA into compact chromosomes. Approximately 147 base pairs of DNA are wounded around an octameric histone core, which consists of H2A, H2B, H3 and H4. This segment of DNA wrapping around a histone core forms a nucleosome. In addition, a linker histone, also known as H1, provides a higher order chromatin organization (12–14). Several subtypes and their function are shortly described in the next paragraph.

H2A has different subtypes, such as H2A.X, H2A.Z, and macroH2A. When DNA damage occurs, H2A.X becomes phosphorylated and facilitates repair mechanisms. H2A.Z acts as a transcription regulator and is linked to both gene activation and gene silencing, depending on the circumstances. MacroH2A is related with transcriptional repression, since it stabilizes the nucleosome. Furthermore, it seems to be associated with blocking cell reprogramming and chromosome X inactivation. H3, forming a central tetramer with H4, is also subdivided, including H3.1, H3.2, H3.3 and centromere protein A (CENP-A). The latter plays a crucial role in the formation of the centromere of chromosomes. The importance of H3 in terms of gene regulation are more specifically described in the next section (12–14).

1.1.4.2. PTMs

Post translational modifications (PTMs) occur when a protein is synthesized. These modifications lead to either irreversible proteolytic cleavage of peptide bonds or reversible covalent addition of chemical groups to amino acids (15,16). Modifications of histones, also known as histone PTMs (hPTMs), are key regulators of epigenetic alterations. These globular proteins contain tails, namely N-terminal regions, which are densely populated with arginine (R), lysine (K), hydroxyl group-containing serine (S), tyrosine (Y) and threonine (T) residues. Adding or removing chemical groups to these tails can potentially cause alteration in the histone-DNA interaction, chromatin organization and thus transcriptional regulation. Furthermore, some hPTMs serve as a recognition site for regulatory proteins, which either modify the chromatin structure or directly influence cellular processes. It is important to note that most of these reactions are catalyzed by enzymes, which are classified as either writers or erasers. Writers are responsible for adding chemical groups, whereas erasers catalyze the removal of these groups. As shown in **figure 1.2**, the most common hPTMs are acetylation and methylation of K, phosphorylation of S and T and ubiquitylation of K (17,18). Combinations of these PTMs on a certain peptide give rise to so-called peptidoforms. These are peptides with an identical amino acid sequence but with a different combination of PTMs (19).

Acetylation of K is catalyzed by histone acetyltransferases (HATs) and erased by histone deacetylases (HDACs), which regulates the chromatin structure as shown in **figure 1.2**, since acetylation neutralizes the positive charge of the lysine side chain. Likewise, acetylation is associated with indirect activation of transcription, by facilitating the recruitment of RNA polymerase and coregulators (20).

Methylation of K and R residues is another important hPTM. Arginine can be monomethylated or dimetyhlated, whereas lysine can also be trimethylated. This modification is catalyzed by histone methyltransferases and histone demethylases and can either activate or inhibit transcription. For instance, methylation of histone 3 lysine 9 (H3K9), H3K27 and H4K20 are mostly related to gene suppression, whereas methylation of H3K4, H3K36 and H3K79 are commonly correlated with gene activation (20).

Phosphorylation of S and T is controlled by kinases and phosphatases, which add and remove negatively charged phosphate groups, respectively. There are three crucial functions of phosphorylated histones, namely; DNA damage repair, control of chromatin structure and regulation of gene expression. One of the specific histone target sites of kinases is H3S10, whereby phosphorylation of this serine leads to a more condensed chromatin state. Furthermore, as mentioned before, phosphorylation of S139 of H2A.X ensures DNA-repair mechanisms (21,22).

Histone ubiquitination is carried out by ubiquitin ligases and can be removed by deubiquitinating enzymes. Monoubiquitylation contributes to protein translocation, DNA damage signaling and transcriptional regulation. For instance, monoubiquitinated H2A (H2AUb) leads to gene silencing, whereas H2BUb induces both transcription activation and inactivation (21,22).

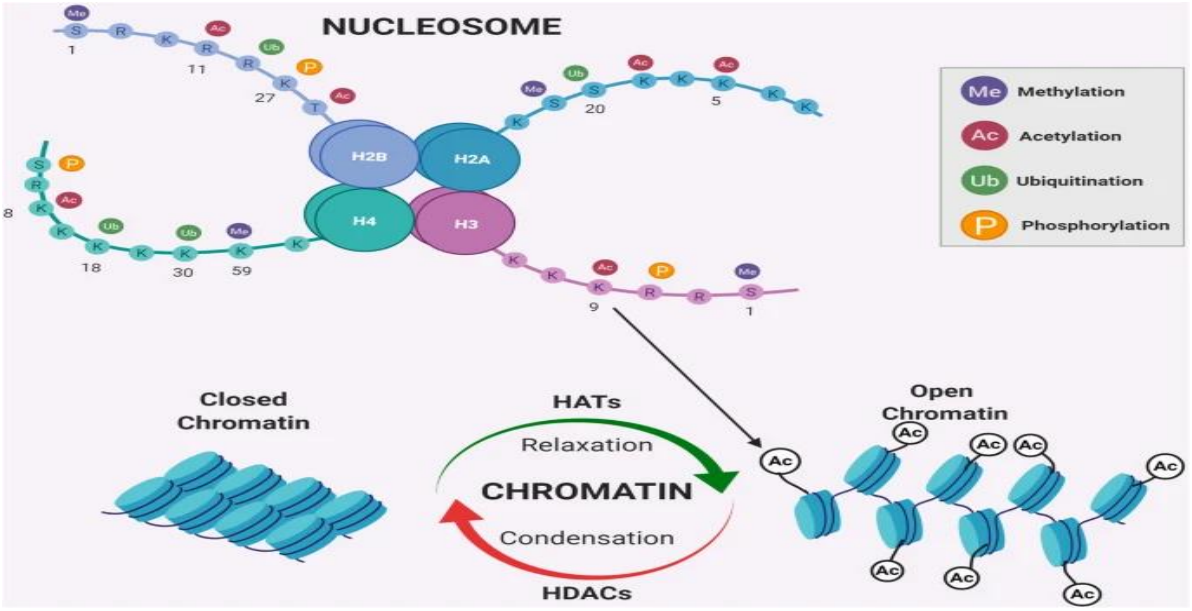

Figure 1.2: Nucleosome consisting of histones with modifiable N-tails. Main modifications are methylation, acetylation, ubiquitination and phosphorylation. Acetylation of K and R catalyzed by HATs leads to open euchromatin structure, whereas deacetylation catalyzed by HDACs provides closed heterochromatin structure (23).

1.2. HISTONE ANALYSIS

Analytical techniques used in the analysis of hPTMs can be classified as antibody-based or mass spectrometry (MS)-based approaches (24).

1.2.1. Antibody-based approaches

Antibody-based methods, such as Western blotting, flow cytometry and protein microarrays, are based on generation and use of protein specific antibodies to investigate the proteome. However, these approaches have some important downsides. Despite the high sensitivity, these conventional methods are unable to disclose combinatorial PTMs patterns. Moreover, as mentioned before, some histone variants are so similar, also known as isoforms, so that antibodies cannot distinguish between them. In addition, PTMs within the same histone can cause blocking of the antibody recognition site of a co-occurring PTM. On top of these specificity problems, limitation of high-throughput is an additional disadvantage (17,24–26).

1.2.2. LC-MS/MS

Liquid chromatography coupled to tandem mass spectrometry (LC-MS/MS) is widely used for analyses of biopolymers and avoids the above-mentioned issues. LC enables separation of the samples based on the interaction with the mobile and the stationary phases, whereas MS determines the molecular mass of the eluents using their mass-to-charge ratio (m/z). In the LabFBT, reversed phase high performance liquid chromatography (RP-HPLC) is used for separation of the different histones whereby the stationary phase is non polar and the mobile phase is polar. This separation is facilitated by the hydrophilic character and high solubility of histones. Following LC separation, analytes are transferred into the mass spectrometer, which is composed of three basic components; i.e. an ion source, a mass analyzer and a detector (24,27–29). During this master dissertation, use was made of a publicly available hPTM atlas of 21 T-ALL cell lines, measured via LC-MS/MS. The MS data was obtained on a TripleTof 6600 instrument (Sciex), consisting of electron spray ionization (ESI) as an ion source, a quadrupole time-of-flight (Q-TOF) as a mass analyzer and an electron multiplier as a detector. Therefore, these components will be further discussed in detail in the following paragraphs.

1.2.2.1. Construction

Ion source

ESI is a soft ionization method used for liquid samples. The LC-eluent leaves the RP-column and enters the ion source by infusing the sample into a narrow metal capillary. A high voltage of several kilovolts (kV) is applied between the end of the capillary and the counter electrode. Consequently as shown in **figure 1.3**, a solution cone, also known as the Taylor cone, is formed at the tip of the capillary. Subsequently, the cone disperses into a spray of charged electrospray (ES) droplets. The charged droplets, which are repelled from each other by the repulsive forces, migrate towards the counter electrode with an opposite charge. At the same time, the size of the droplets diminishes by solvent evaporation with the help of heated dry gas. Eventually, gas-phase analyte ions are formed, which enter the mass analyzer (30–32).

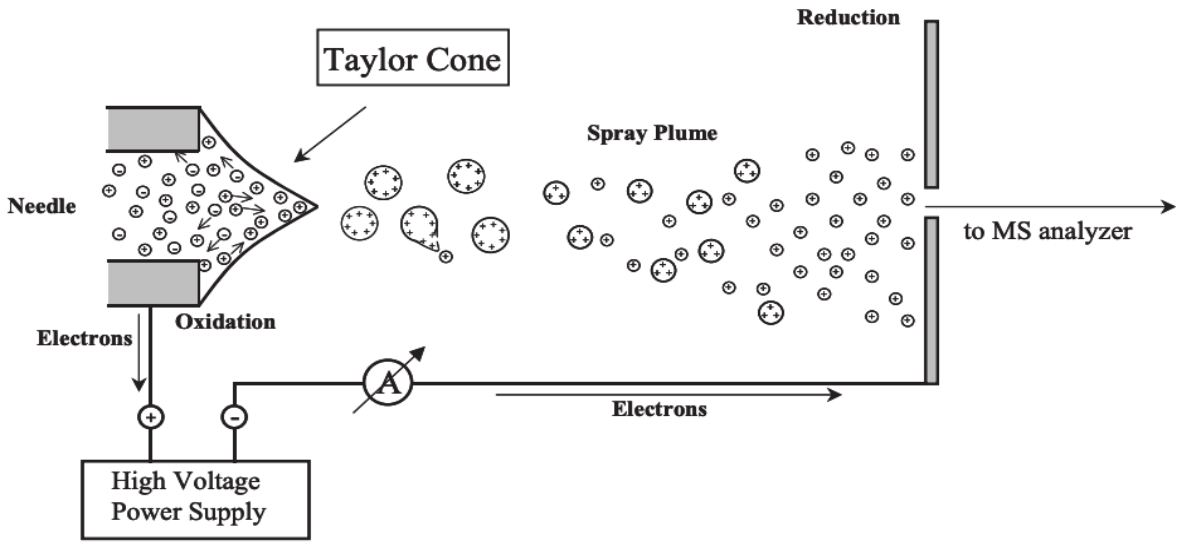

Figure 1.3: ESI, whereby the Taylor cone is formed with the help of high voltage between the capillary needle and the counter electrode. Thereafter charged droplets arisen from the cone move towards the oppositely charged side whilst decreasing in size. Finally, naked ions in gaseous phase enter the mass analyzer (32).

Mass analyzers

Q-TOF is a combination of two different mass analyzers and consists of three compartments as illustrated in **figure 1.4**, namely two quadrupoles Q1 and Q2, followed by a time-of-flight (TOF) tube. The first quadrupole Q1 acts as a mass-filter for the selection of ions based on their mass-to-charge ratio (m/z). The specific m/z selection is possible due to four parallel circular rods, where each opposite rod is connected electrically. Direct current (DC) and radiofrequency (RF) potentials are applied to each pair of rods leading to a controlled oscillation of the ions. Only the ions with stable trajectories will surpass Q1 and enter the subsequent Q2. Q2 is a collision cell, which ensures fragmentation of the ions by collision induced dissociation (CID). Afterward, the fragmented product ions are transferred into the ion pulser of the TOF, where all ions obtain the same kinetic energy and accelerate perpendicular to their initial direction. The ions with a lighter mass will have a shorter time of flight, while the heavy ions will take longer before reaching the detector (33,34).

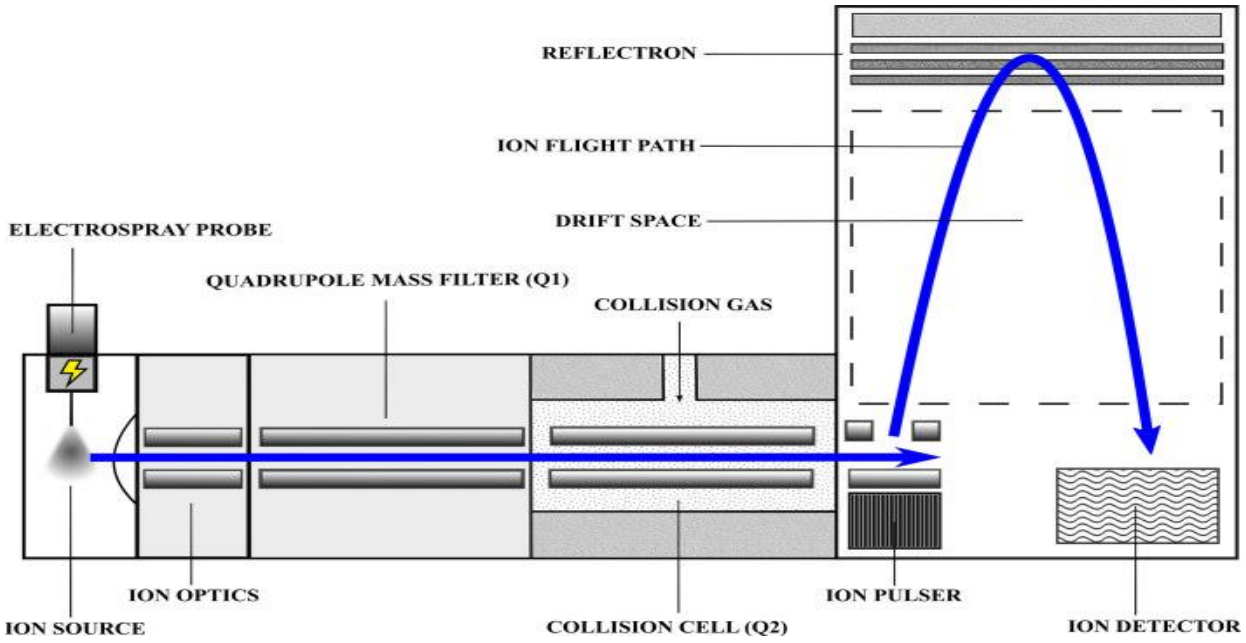

Figure 1.4: Schematic diagram of a Q-TOF mass spectrometer composed of three main components, namely Q1, Q2 and TOF. Q1 acts as a mass filter and Q2 is responsible for the further fragmentation of precursor ions into product ions. Finally, the mass of the product ions is analyzed based on their time of flight (33).

Ion detector

Detection of ions by current measurement is commonly accomplished by using an electron multiplier (EM), which consists of either discrete dynodes or continuous dynode. Microchannel plate (MCP), which is a variant of the continuous dynode EM, is a widely used detector. As shown in **figure 1.5**, it is comprised of 10^4 - 10^7 parallel oriented micro channels in a disk-shaped device where both sides are coupled by electrodes. The electrons strike the continuous dynode in the microchannels causing secondary electrons, which in turn strike other dynode surfaces resulting in electron amplification. Eventually, the electron multiplication leads to an increase in signal with a factor of 10^4 – 10^7 (35,36).

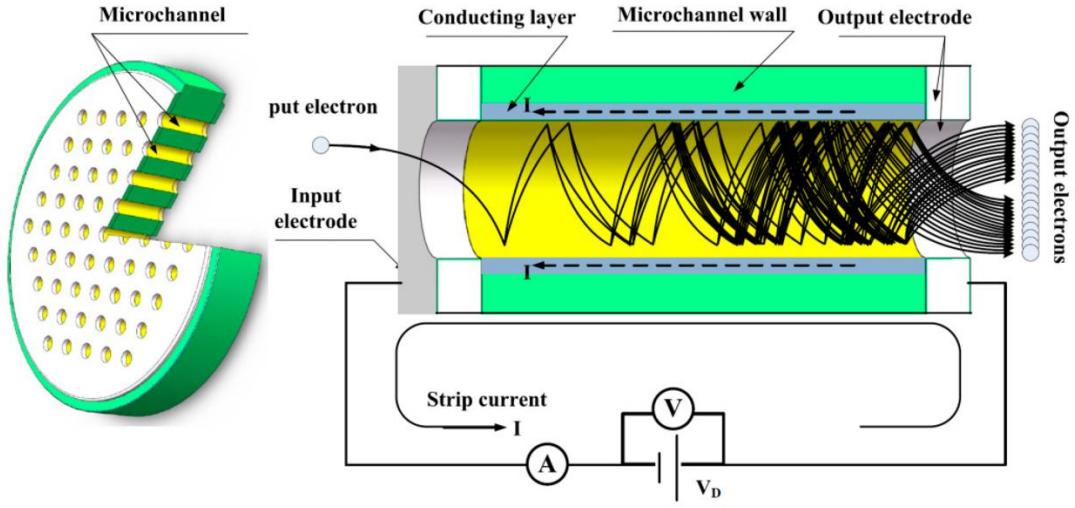

Figure 1.5: Schematic representation of MCP, whereby electrons are multiplied into secondary electrons with the help of dynodes. The amplified secondary electrons beam from the other side of the microchannel resulting in an increased signal (37).

1.2.2.2. MS-based approaches

As shown in **figure 1.6**, MS-based analysis of histones can be divided into three main approaches, bottom-up, middle-down and top-down methods. Bottom-up approach includes proteolytic cleavage of histones into smaller peptides, which are detected by MS/MS detector. However, co-elution of short isobaric peptides is not uncommon and thus leads to problems in terms of data analysis. In addition, digesting proteins to peptides can cause a lot of information loss. Alternatively, middle-down and top-down methods are tackling these issues due to detecting respectively larger peptides and intact proteins. The middle-down method is based on cleaving the N-tail of proteins generating larger peptides compared to the bottom-up strategy, which results in maintaining the majority of hPTMs. As mentioned before, top-down method is based on characterization of intact proteins providing faster sample preparation, given that digestion is not required. Moreover, the top-down approach ensures a more extensive overview of the histone code. Despite the advantages, this method requires high resolution tandem mass analyzers and more advanced software, since more complex MS or MS/MS spectra are generated (27,38).

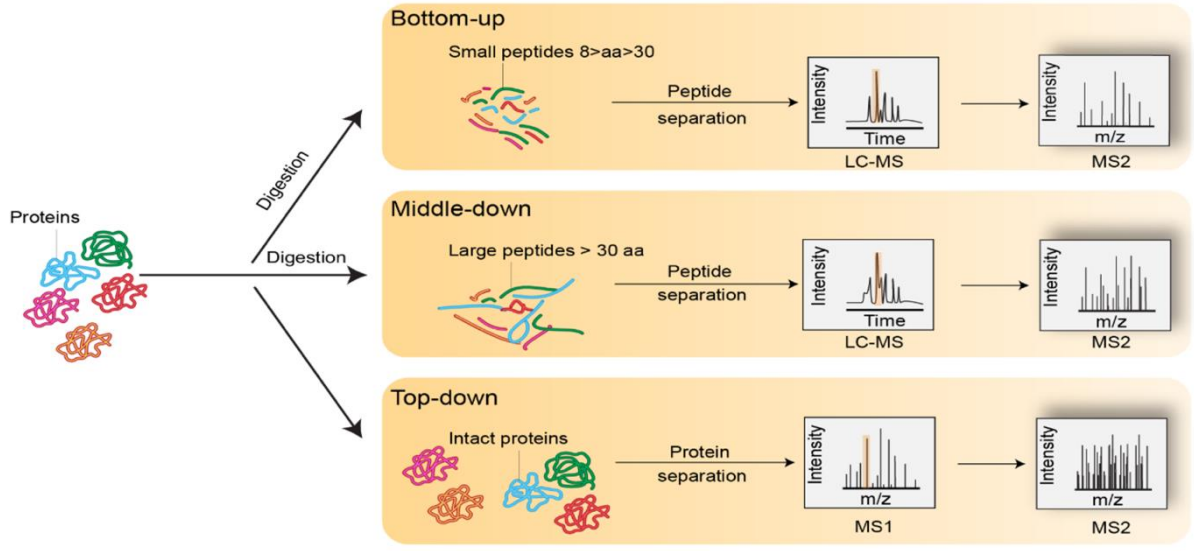

Figure 1.6: The three main MS-based approaches: Bottom-up, middle-down an top-down. Unlike top-down methods, digestion is required for bottom-up and middle-down methods, forming respectively small peptides and large peptides (17).

1.2.2.3. Data acquisition

Data acquisition can either be targeted, including parallel monitoring (PRM) and selected reaction monitoring (SRM) or non-targeted. The non-targeted approaches can be subdivided in two main groups, namely data dependent acquisition (DDA) and data independent acquisition (DIA). The hPTM atlas used in this master dissertation was generated using DDA, which is shortly described in the next paragraph (33,39).

Data dependent acquisition (DDA) is a non-targeted data acquisition mode based on selection of precursor ions from MS scans according to pre-selected criteria (40). As illustrated in **figure 1.7**, in DDA, the intact ions are detected before fragmentation in the collision cell, whereafter the most-intense precursor ions are selected for further fragmentation. In essence, a full mass spectrum (MS1) is generated before fragmentation, followed by formation of a tandem mass spectrum (MS2) after fragmentation of selected ions (33,39).

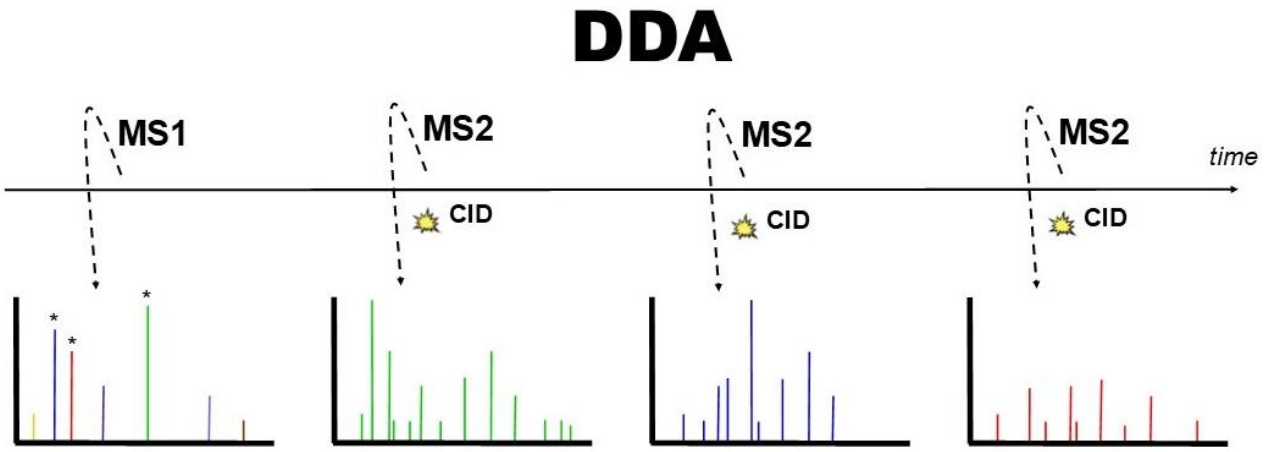

Figure 1.7: First, an intact precursor ion scan (MS1) is generated, followed by isolation and fragmentation of the most abundant precursor ions. This selected fragmentation of precursor ions generates tandem mass spectra (MS2) (41).

1.2.2.4. Data analysis

Data analysis of hPTMs consists of both identification and quantification. For protein identification, database searching was used, which is an in silico method. There are four main approaches for database searching, namely peptide mass fingerprint, peptide sequence tag search, spectral library search and MS/MS ion search (42). The latter approach is applied for this master dissertation, whereby protein sequences in a database are digested in silico followed by fragmentation, generating theoretical MS/MS spectra. Thereafter, the experimentally obtained MS/MS spectra are compared to these generated theoretical MS/MS spectra for peptide and PTM identification. The certainty of the identification is indicated by a score, such as the Mascot delta score (24,42).

Quantification of peptides is either label-based or label-free. Label based quantification is based on isotope tags incorporating within peptides, including TMT and ITRAQ labeling, which is commonly used for absolute quantification (43). In contrast to label-based, label-free quantification is mostly used for relative quantification and is based on either spectral counting of peptides or visualizing the intensity of the peaks. Spectral counting involves the relative quantification of proteins between samples, whereby the number of spectra is proportional to the amount of proteins presented in the samples. The second approach for label-free quantitation, which was used in the hPTM atlas, involves visualizing the intensity of peaks as a function of the retention time in an extracted ion chromatogram (XIC). Consequently, the area under the curve (AUC) can be determined, which is correlated with the protein abundance (24,42,44,45).

1.3. EPIGENETICS IN CANCER

1.3.1. General principles

Differentiation of cells into unique cell types depends on silencing and activation of specific genes, which results in a unique pattern of gene expression. The control of gene expression and the fate of cells is to a large extent regulated by epigenetic mechanisms. Aberration in these mechanisms, mainly DNA methylation, hPTMs and ncRNA leads to uncontrolled development of cells, eventually causing cancer. Some epigenetic modifications correlated with cancer are described in the following paragraphs (46–48).

As shown in **figure 1.8**, during carcinogenesis, initially active genes can become silenced by DNA hypermethylation with cooperation of H3K9 methylation. For example, when tumor suppressor gene (TSG) promotors with CpG sites become methylated and thus inactive, which in turn promote cancer. Another way of silencing active genes, is via overexpression of Polycomb Repressive Complex (PRC). PRC is a protein complex, which catalyzes the formation of H3K27 methylation and H2Aub (49). Both H3K27 methylation and H2Aub play an essential role in terms of gene repression. As mentioned before, H2A.X plays a crucial role in DNA-repair mechanisms, which is also used to kill cancer cells. When a DNA double strand break occurs, H2A.X accumulates at the break site and becomes phosphorylated. As a result, proteins involved in DNA repair accumulate (50). Finally, it is important to note that in contrast to silencing, activation of originally silenced genes can also occur, which also alters the gene expression pattern. For instance, hypomethylation of oncogenes and global DNA hypomethylation contribute to the overexpression of genes, which can lead to tumorigenesis (51–53).

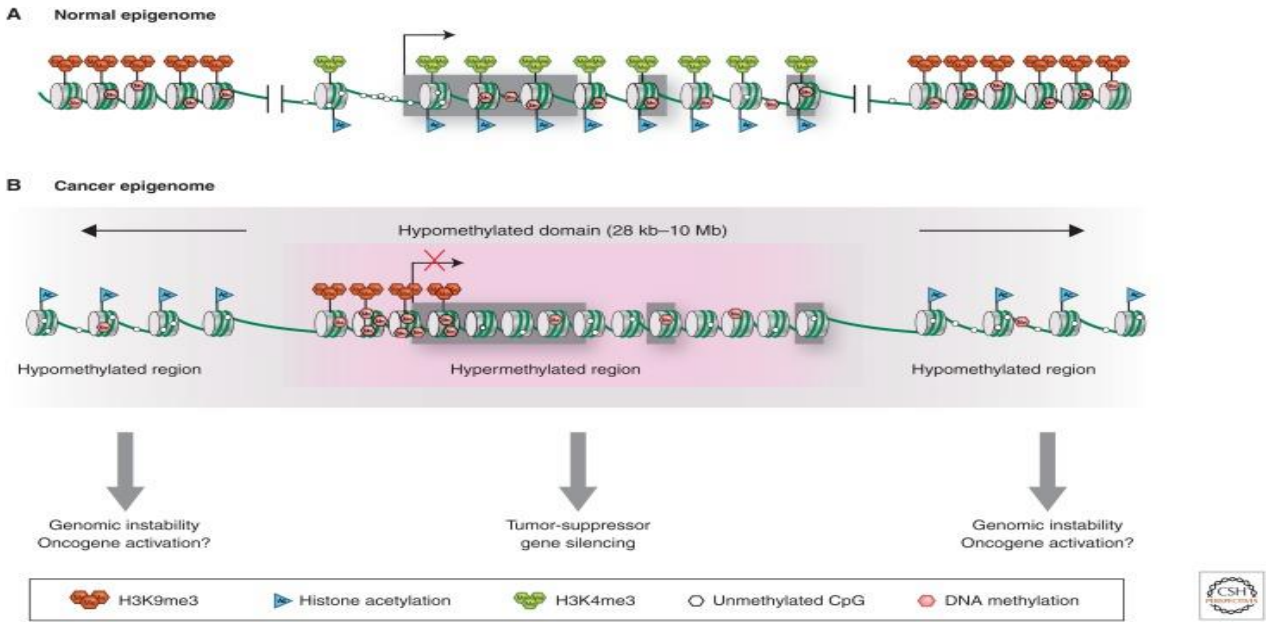

Figure 1.8: A) Epigenome of a normal cell, where non-coding regions are suppressed by H3K9me3 and DNA methylation. The hypomethylated active genes are marked by H3K4me3 along with histone acetylation. B) Epigenome of a cancer cell, with a global loss of DNA methylation interspersed with abnormal hypermethylated regions and H3K9me3 (53).

Dysregulation in the expression of miRNAs has been reported in several cancers, including leukemia, lung cancer, prostate and bladder cancer. These small ncRNA's can function as either tumor suppressors or oncogenes depending on their target complementary strands. Most tumor suppressor miRNAs targeting growth-promoting genes are inactive in cancer, whereas oncogenic miRNAs targeting growth-inhibitory genes are commonly upregulated. Epigenetic alteration, in particular DNA methylation, is one of the reasons for silencing the tumor suppressor miRNAs (52).

1.3.2. T-ALL

T-cell acute lymphoblastic leukemia (T-ALL) is an aggressive hematological cancer, whereby oncogenes and tumor suppressor genes are dysregulated. T-ALL appears more often in males than females and comprises of around 15% of pediatric and 25% of adult ALL cases. For current treatments, cure rates in childhood T-ALL are around 85%. Unlike childhood T-ALL, the clinical outcome for adult T-ALL is remarkably different with a survival of less than 50%. Moreover, current treatment protocols consist of high-dose combination therapy, which commonly result in short-term and long-term side effects. In addition, a significant number of patients relapse and show poor treatment response. For example, an increased nucleotidase activity was observed in T-ALL causing resistance to chemotherapeutics such as 6-mercaptopurine. Considering these issues, newer therapies and more advanced treatment stratification are required (54,55).

In the recent past, studies have shown the involvement of more than 100 mutated genes in T-ALL. Only two of these genes, namely NOTCH1 and CDKN2A/2B, are mutated in more than 50% of T-ALL. Furthermore, T-ALL is subdivided into subgroups based on immunophenotyping, which uses antibodies identifying protein markers on the surface of the cells (56). In a landmark study, Huether et al. sequenced 633 epigenetic regulatory genes in more than 1000 pediatric tumors and demonstrated that T-ALL has the most mutated epigenetic regulatory genes among all tumors. This suggests that epigenetic alterations are highly common in T-ALL, including DNA methylation and histone post-translational modifications (54,55).

Changes in the expression of different miRNAs are common in T-ALL. Oncogenic miRNAs downregulate tumor suppressor genes, whereas other miRNAs cause overexpression of oncogenes. Moreover, some T-ALL types are characterized by altered lncRNA expression, which suggests its importance in the differentiation of T-cells (54). In the next paragraph some examples of epigenetic regulation in T-ALL is described.

As shown in **figure 1.9**, PRC2, including EZH2, SUZ12 and EED, methylates H3K27 forming the repressive mark H3K27me3. This enzyme complex has a tumor suppressor role and its downregulation has been reported in T-ALL. The loss of PRC2 and thus H3K27me3 may be explained by the activation of the oncogenic NOTCH1 gene. NOTCH1 leads to disruption of PRC2 and recruitment of lysine demethylases 6B (KDM6B, also named JMJD3), which in turn cause downregulation of H3K27me3. The overexpression of JMJD3 may be correlated with the maintenance of oncogenic NOTCH1 activation. Furthermore, lysine demethylases 6A (KDM6A, also called UTX) also cause downregulation of H3K27me3 and activation of genes. Likewise, UTX is a member of the MLL2 complex, which methylates H3K4 and activates gene transcription. Although UTX and PRC2 have opposite functions on gene transcription, both acts as tumor suppressors. This is possible given that both affect different genomic loci during T-cell differentiation. A more recent study showed the importance of two enzymes, namely NSD2 and SETD2 in T-ALL. Both enzymes catalyze the methylation of H3K36, which is associated with gene activation. Moreover, NSD2 is mutated in multiple T-ALL cell lines, such as HPB-ALL, RPMI-8420 and MOLT-13, which further confirms the functional importance of H3K36 methylation (55,57).

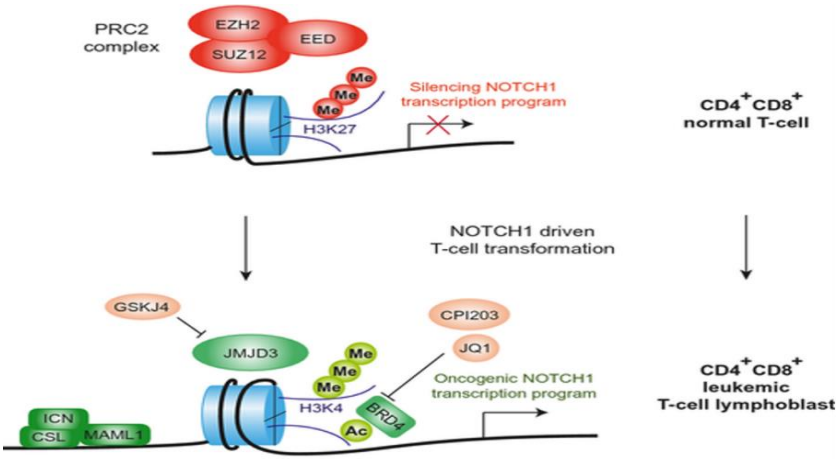

Figure 1.9: Activating NOTCH1 transcription results in transformation from normal T-cell to lymphoblastic T-cell. Originally low levels of NOTCH1 signaling occurs in normal cells due to the presence of repressive PRC2 and H3K27me3. Epigenetic alterations, such as H3K4 methylation, H3K27 demethylation cause NOTCH1 activation. As a result, downregulation of PRC2 complex and loss of H3K27me3 with the recruitment of JMJD3 occurs (55).

1.4. EPIDRUGS

1.4.1. General/Classes

The increasing knowledge on epigenetic variations in different cancers led to the development of new targeted therapies for cancer treatment. Epidrugs, which are modifying the DNA and chromatin structure, can restore these reversible epigenetic alterations in cancer, which makes these alterations an interesting target. The mode of action mainly comprises controlling enzymes, reactivating silenced tumor suppressor genes and facilitating DNA repair mechanisms. Furthermore, epidrugs can either be used i) in monotherapy as a cytotoxic agent or ii) in combination therapy as a sensitizer, thereby lowering drug resistance (51,58). As shown in **figure 1.10**, epidrugs can currently be classified into five groups, namely DNA methyltransferase inhibitors (DNMTi), histone deacetylase inhibitors (HDACi), histone methyltransferase inhibitors (HMTi), histone demethylase inhibitors (HDMi) and Bromo and extra terminal domain inhibitors (BETi) (58). In this master dissertation, the response of 21 T-ALL cell lines to HDACi and DNMTi was investigated, which are described in the following section.

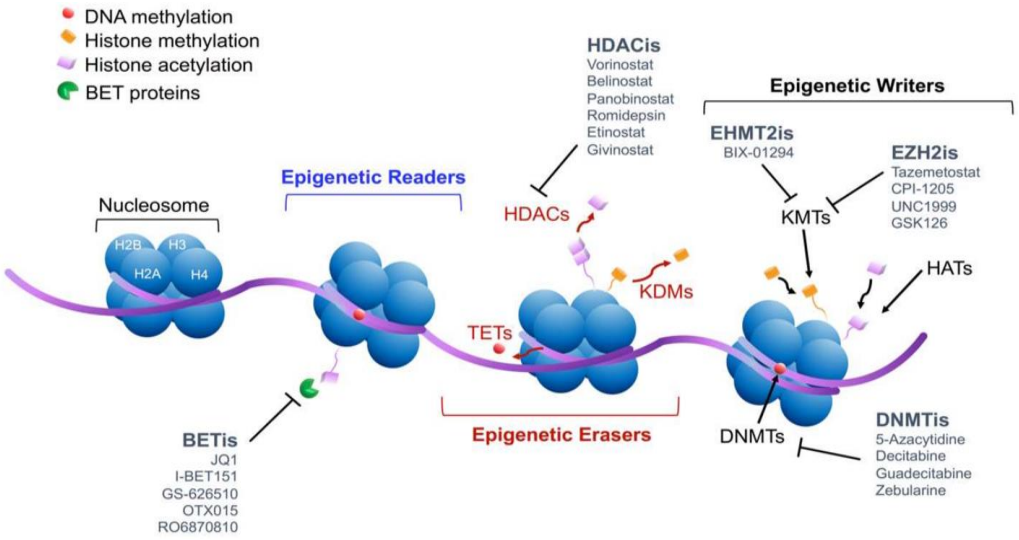

Figure 1.10: Illustration of a nucleosome with epigenetic modifications, including DNA methylation and histone modifications. Epidrugs tested in preclinical or clinical settings are shown in grey (59).

1.4.2. DNMTi

Altered patterns of DNA methylation in cancer can be reversed by DNMTis, which can be subdivided in nucleosides, including azacytidine (AZA) and decitabine (DAC), and non-nucleosides, such as GSK3685032. Nucleoside analogs incorporate into DNA at cytosine residues where they covalently bond with DNMTs, resulting in depletion of cellular DNMT. Moreover, contrary to GSK3685032, nucleoside DNMTis commonly have off-target effects, causing dose-limiting toxicity. Unlike the nucleoside analogs, the structures of non-nucleosides are more heterogeneous and their mode of action is independent of DNA incorporation. Some non-nucleoside DNMTis act by binding directly the active site of enzymes, although many act by unknown mechanisms (60–63). Both nucleoside and non-nucleoside analogs inhibit CpG methylation and thereby restore silenced genes. In this master dissertation three DNMTi compounds were investigated, namely DAC, AZA and GSK3685032. DAC and AZA are currently used as a first-line therapy for the treatment of myelodysplastic syndrome (MDS) when stem cell therapy is contra-indicated. Likewise, it is used for myelomonocytic leukemia and acute myeloid leukemia (AML). GSK3685032 was recently discovered by Pappalardi et al. and showed improved tolerability and efficacy in AML. It can be classified as a highly potent non-nucleoside DNMTi, which is more selective for DNMT1 and less toxic compared to AZA and DAC. Therefore, it seemed promising to test it in T-ALL (51,58,64,65).

1.4.3. HDACi

Altered acetylation and increased HDAC levels have been identified in hematological cancers. HDACis, which potentially reverse the malignant phenotype, can be classified as zinc (Zn^{2+}) and nicotinamide adenine dinucleotide (NAD+) dependent deacetylase inhibitors, whereby the latter is also known as sirtuin inhibitors (SIRTis). Both classes of epidrugs prevent deacetylation by blocking the catalytic site of HDAC, which causes hyperacetylation and thus gene activation (51,58,64,66,67). In this master dissertation three HDACi compounds were investigated, namely panobinostat, romidepsin and vorinostat. Panobinostat in combination with bortezomib and dexamethasone is used for the treatment of multiple myeloma. Romidepsin and vorinostat are indicated for the treatment of Cutaneous T-cell lymphoma. The six different drugs used for this master dissertation with the corresponding indication, mode of action and clinical status are shown in **table 1.1** (51,58,64,65).

Table 1.1: Epidrugs used with corresponding treatment indication and status (51,68–71)**.**

Class	Epidrug	Treatment indication	Status
DNMTi	Azacytidine	Monotherapy: Myelodysplastic syndrome Combination therapy (+ decitabine or low dose cytarabine): Acute myeloid leukemia	Approved
DNMTi	Decitabine	Monotherapy: Acute myeloid leukemia	Approved
DNMTi	GSK3685032	-	Not approved
HDACi	Panobinostat	Combination therapy (+ Bortezomib + Dexamethasone): Multiple myeloma	Approved
HDACi	Romidepsin	Cutaneous T-cell lymphoma	Approved
HDACi	Vorinostat	Cutaneous T-cell lymphoma	Approved

1.5. PERSONALIZED MEDICINE

1.5.1. General principle

Current health care practices are commonly based on standard treatments applied to every individual. However, these individuals respond differently to the same drug, which can result in either subtherapeutic or undesired effects. The uniqueness in drug response among the population is caused by genetic differences, which is studied by pharmacogenetics, as well as epigenetic variations, which is studied by pharmacoepigenetics. The latter can be impacted by living conditions, health and lifestyle leading to aberrations in gene expression. Eventually, genes encoding for metabolism, transporters and receptors can be altered or epigenetically modified providing unfavorable effects. For example, epigenetically acquired drug resistance leading to chemotherapeutic failure is a common problem in cancer treatment. This resistance can be explained by increased drug efflux, drug target mutations, decreased bioactivation or decreased drug uptake (4,71,72).

The above mentioned issues can be avoided if the variations in gene expression responsible for the aberrant drugs responses, are identified. Once identified, genetic and epigenetic alterations can be used as predictive biomarkers. The usage of these biomarkers contributes to personalized medicine, which is clarified in the section 1.5.2. Pharmacoepigenetics.

1.5.2. Pharmacoepigenetics

Pharmacoepigenetics studies the epigenetic basis for individual variation in drug response and has the potential to become an important element of personalized medicine. A key player determining the response to a particular drug are the drug metabolizing enzymes and transporters (DMETs). Alterations in DMET gene expression are mainly caused by changes in DNA methylation, histone modifications and miRNA (73).

For example in T-ALL, mutations in SETD2, which catalyzes H3K36 methylation, cause resistance to DNA damaging chemotherapeutics. Treatment with HDMi, restores the methylated H3K36 levels and thus the sensitivity to the drugs. A second example, in colon cancer, is the pregnane X receptor (PXR), which is activated by different lipophilic xenobiotics, including chemotherapeutics. PXR binds to DNA and regulates genes responsible for detoxification and excretion of substances. Furthermore, PXR regulates drugs metabolizing enzymes such as CYP3A and influences the intestinal first-pass metabolism. DNA methylation in the promotor of the PXR genes cause inactivation and downregulation of the CYP3A enzymes, whereas hypomethylation provides upregulation of CYP3A4. This variation in DNA methylation in the promotor of PXR genes partly explains the inter-individual difference of drugs response in colon cancer (74,75).

Given that these epigenetic alterations play a crucial role in drug response, epigenetic biomarkers can be used for diagnostic and prognostic purposes. An example of an epigenetic biomarker in childhood ALL is miRNA, which can be used for diagnosis, classification and prediction of prognosis. Some oncogenic miRNAs are upregulated, whereas some tumor suppressor miRNAs are downregulated (see appendix table 1). Another ncRNA, namely lncRNA, seems to have an important role in cancer development as well, and can be used for classification of cancer subtypes and stratification of patients (76). DNA methylation patterns can also be used as biomarkers, given that alterations in these patterns occur during the progression of leukemia and affect clinical outcome. In contrast to the older studies on methylation patterns in T-ALL published by Roman-Gomez et al. (77,78), more recent studies have shown better clinical outcome when DNA is hypermethylated. Moreover, poor prognosis was observed in hypomethylated T-ALL. However, the clinical meaning of DNA methylation patterns in T-ALL remains unclear (73,76,78–80).

Current drug treatment of T-ALL is based on antimetabolites, alkylating agents, microtubule-destabilizing agents, anthracyclines, nucleoside analogues and hydrolyzing enzymes. Furthermore, stratification of the patients as standard-, medium-, or high-risk groups is based on the minimal residual disease (MRD) and response to steroids given in pre-treatment. As mentioned before in section 1.3.2. T-ALL, these current treatment protocols deal with relapses, therapy resistance and side effects. Therefore, more targeted therapies are required, including other molecular biomarkers in addition to the current MRD detection. In this master dissertation, correlation between hPTM profiles and drugs responses in 21 different T-ALL cell lines are investigated, whereby the hPTMs can be potentially used as predictive biomarkers and the epidrugs as co-medication when therapeutic resistance occurs (81).

2. OBJECTIVES

The crucial role of epigenetics in T-ALL, including drug resistance, is increasingly confirmed by scientific studies (55,76,78,79). In some T-ALL subtypes, even after consolidation of the current treatments, resistance and relapse occur. Moreover, raising the dose to compensate for drug resistance is not always applicable, given that these treatment protocols lead to dose-dependent toxicities. Considering these issues, better T-ALL patient stratification and new targeted therapies are required. Epigenetic modifications, which cause changes in the chromosome without altering the DNA sequence, are interesting targets, since they plays a crucial role in gene expression and thus cell phenotype. In addition, unlike genetic mutations, epigenetically acquired resistance driven by hPTMs and DNA methylation, can be reversed by so called epidrugs. The objective of this master dissertation is to link the dose-response of 21 T-ALL cell lines to six different epidrugs to their baseline hPTM levels.

First, the 21 cell lines will be treated with a dilution series of the six drugs and cell viability will be measured using Cell Titer Glo. Then, I will plot the viability data in survival curves and determine the IC50 and AUC for each drug. Finally, I will link the IC50 and AUC values of each cell line with their respective hPTM levels using Spearman correlation and Principal Component Analysis (PCA). To do this, I will use a hPTM atlas of each cell line obtained by Provez et al., which is publicly available to the community as a Progenesis QIP project. Eventually, if there is a correlation between hPTMs and drug response, hPTMs can be used as predictive biomarkers, which further contributes to personalized treatment.

However, when a significant correlation between one or a combination of hPTMs and drug response is found, further validation is needed in the future. hPTMs of interest can be removed by either knock out or pharmacological inhibition of the writer of the PTM, whereafter the results either confirm or contradict the initial observations. Accordingly, co-treatment with other epidrugs increasing the sensitivity of the cell lines to a particular drug can be examined.

3. MATERIALS AND METHODS

Table 3.1: Materials used during this master dissertation

Product	LOT	Model	Serie-Nr.	Manufacturer
Azacytidine	S178207	-	-	Selleckchem
Decitabine	S120010	-	-	Selleckchem
Panobinostat	S103012	-	-	Selleckchem
Romidepsin	S302003	-	-	Selleckchem
Vorinostat	S104712	-	-	Selleckchem
GSK3685032	E104601	-	-	Selleckchem
Centrifuge	-	Megafuge ST4R Plus	42779322	Thermo Fisher
Incubator	-	INCU-Line IL 56 Prime	IL56S 160056	VWR
CO_2 incubator	-	MCO-230AICUV-PE	180960087	PHCbi
Plate reader	-	GloMax Explorer Promega	9720000038	Promega
Cell counter	-	Countess™ II FL Automated Cell Counter	AMQAF1000	Thermo Fisher
Microscope	-	EVOS Floid Imaging System	4471136	Thermo Fisher
DMSO	-	-	67-68-5	Gibco
Trypan blue	-	-	T10282	Life technologies
RPMI medium	2339167	-	52400041	Gibco
L-glutamine	-	-	25030024	Gibco
Penicillin Streptomycin	-	-	15140122	Gibco
Beta-mercaptoethanol	-	-	31350010	Gibco
Non-essential amino acids	-	-	11140050	Gibco
Sodium pyruvate	-	-	11360070	Gibco
CellTiter-Glo	0000510589	-	G7572/G7573	Promega
PBS	2156430	-	20012027	Gibco

3.1. CELL CULTURE

As shown in **table 3.2**, The 21 T-ALL cell lines were purchased from different labs, and grown in RPMI 1640 medium (Gibco, Thermo Fischer, UK) supplemented with penicillin, streptomycin, L-glutamine and 10% or 20% fetal calf serum (FCS) depending on cell line (see table 3.2). For PER-117, other medium was used, namely RPMI 1640 containing 10% FCS, non-essential amino-acids, sodium pyruvate and 50 nM of beta-mercaptoethanol. Subsequently, cell cultures were incubated at 37°C with 5% CO_2 and 95% humidity (PHC corporation, Etten Leur, The Netherlands). Cultures were verified to be free of mycoplasma contamination using the TaKaRa PCR Mycoplasma Detection kit.

3.1.1. Splitting

The cell cultures were split twice a week to maintain a cell density of $0{,}6.10^6$ cells/mL or $0{,}8.10^6$ cells/mL depending on the cell line, except PER-117, which has a desired cell density of $0{,}25.10^6$ cells/mL (see table 3.2). First, culture flasks were visually checked for cell density and contamination using a light microscope (ThermoFisher, EVOS floid imaging system). Subsequently, 10 µL of the cell suspension was mixed with 10 µL trypan blue and cells were counted in an automated cell counter. Finally, the volume of fresh medium needed to attain the required cell density was added.

Table 3.2: Overview of the 21 T-ALL cell lines used with their required % FCS and optimal cell density (82)**.**

Cell line	Required % FCS	Required cell density (10^6 cells/mL)	Origin	Year	Purchased from
HSB-2	10%	0,8	The peripheral blood of an 11-year-old boy with ALL	1966	DSMZ
PEER	20%	0,8	The peripheral blood of a 4-year-old girl with T-ALL	1977	DSMZ
JURKAT	10%	0,6	The peripheral blood of a 14-year-old boy with ALL	1976	DSMZ
MOLT-16	20%	0,8	The peripheral blood of a 5-year-old girl with T-ALL	1984	DSMZ
LOUCY	10%	0,6	The peripheral blood of a 38-year-old woman with T-ALL	Unknown	DSMZ
RPMI-8402	10%	0,8	The peripheral blood of a 16-year-old woman with ALL	1972	DSMZ
HPB-ALL	20%	0,8	The peripheral blood of a 14-year-old boy with ALL	1973	ATCC
TALL-1	20%	0,8	The peripheral blood of a 28-year-old man with lymphosarcoma	1976	DSMZ
SUP-T11	10%	0,8	The bone marrow of a 74-year-old man with T-ALL	Unknown	DSMZ
PF-382	10%	0,8	The pleural effusion of a 6-year-old girl with ALL	Unknown	DSMZ
PER-117	10%	0,25	Unknown	Unknown	Richi Kotecha's Lab
P12-ICHIKAWA	20%	0,8	The peripheral blood of a 7-year-old boy with ALL	Unknown	DSMZ
MOLT-4	20%	0,6	The peripheral blood of a 19-year-old man	1971	DSMZ
KOPT K-1	10%	0,8	Unknown	Unknown	Wendel, Hans-Guido lab
KE-37	20%	0,8	The peripheral blood of a 27-year-old man with ALL	1979	DSMZ
KARPAS-45	20%	0,8	The bone marrow of a 2-year-old boy with ALL	1972	ECACC
DND-41	10%	0,8	The peripheral blood of a 13-year-old boy with T-ALL	1977	DSMZ
CUTTL-1	20%	0,8	Unknown	Unknown	Wendel, Hans-Guido lab
CCRF-CEM	20%	0,8	The peripheral blood of a 3-year-old girl with ALL	1964	DSMZ
ALL-SIL	20%	0,8	The peripheral blood of a 17-year-old man with T-ALL	Unknown	DSMZ
KARPAS-45 JC	20%	0,8	Unknown	Unknown	Lab Jan Cools (KULeuven)

3.2. IC50 DETERMINATION

3.2.1. Cell treatment

To determine the IC50 of azacytidine (S1782, Selleckchem, AZA), decitabine (S1200, Selleckchem, DAC), panobinostat (S1030, Selleckchem, PAN), vorinostat (S1047, Selleckchem, VOR), romidepsin (S3020, Selleckchem, ROM) and GSK3685032 (E1046, Selleckchem, GSK), the 21 T-ALL cell lines were treated with a dilution series of each compound in medium. Before treatment, 2 – 3 million cells from each cell line were centrifuged at 4°C, 1500 RPM for 5 minutes. Then, the supernatants were discarded and the pellets were resuspended in fresh RPMI medium with 10% or 20% FCS depending on the cell line (see table 3.2) to attain around 25000 cells per well. Afterwards, 96-well white plates were prepared by adding 95 µL cell suspension to each corresponding well. Importantly, the empty wells were filled with phosphate-buffered saline (PBS)(Thermo Fisher, UK) to protect against evaporation. For AZA and DAC, each concentration was added daily during four days to assure a constant drug exposure, since the half-life of AZA and DAC is approximately 8-12 hours in vitro (83). For each compound, the dilution series were optimized in order to center the concentration range around the average IC50. The final percentage of vehicle was equal in each concentration point (0.1% DMSO for PAN, VOR, ROM, AZA and DAC; 0.2% ethanol for GSK). The treated cells were incubated for a certain duration depending on the epidrug (see table 3.3) at 37°C with 5% CO_2 (PHC corporation, Etten Leur, The Netherlands). Each cell line was treated twice in the same well plate (two technical replicates) and each treatment was performed thrice on different days (three biological replicates).

Table 3.3: Overview of dilution series and incubation time per drug.

Epidrugs	Dilution series (in 2% DMSO – with exception of GSK in 4% ethanol)	Incubation time (days)
AZA	50 – 10 – 1 – 0,1 – 0,01 – 0 (µM)	4
DAC	50 – 10 – 1 – 0,1 – 0,01 – 0 (µM)	4
GSK	10 – 5 – 1 – 0,5 – 0,1 - 0,01 – 0 (µM)	6
PAN	25 – 10 – 5 – 2,5 – 1 – 0 (nM)	3
VOR	5 – 1 – 0,75 – 0,5 – 0,25 – 0,1 – 0 (µM)	3
ROM	5 – 2,5 – 1 – 0,5 – 0,1 – 0 (nM)	3

3.2.2. Cell viability assay

CellTiter-Glo Luminescent Cell Viability assay was used in this master dissertation, which is a homogeneous method to determine the amount of viable cells based on ATP quantification. By adding the CellTiter-Glo reagent (Promega Corporation, 2800 Woods Hollow Road Madison, USA) to cells, luminescent signals are produced proportional to the amount of ATP and thus the number of living cells. After the preferred incubation time (see table 3.3), 50 µL of CellTiter-Glo reagent was added to each well. Then, the 96 well white plates were shaken for two minutes and incubated in the dark at room temperature for 10 minutes, followed by recording the luminescence at 1500 msec with the plate reader (Promega Corporation, 2800 Woods Hollow Road Madison, USA). The cell viability at each concentration was calculated by taking the average luminescence of the two technical replicates relative to the two technical replicates only containing the vehicle.

3.3. DATA ANALYSIS

3.3.1. Cell viability data

For each cell line, the average luminescence and standard deviation of the three biological replicates were calculated at each concentration in Microsoft Excel. Afterwards, GraphPad prism was used to plot survival curves and to determine the IC50 and AUC values. Plotting the survival curves was performed by using a non-linear regression with the equation; *Asymmetric (five parameter), X is log(concentration)* and IC50s were determined by using non-linear regression with the equation; *absolute IC50, X is concentration*. AUC was determined by using XY analysis with the parameter *area under curve (AUC*).

3.3.2. hPTM correlation

Baseline hPTM profiles of the 21 T-ALL cell lines were determined via bottom-up LC-MS/MS by Provez et al. (84). Briefly, T-ALL cells of each cell line were collected 24 hours after medium was refreshed (six biological replicates). Then, histones were extracted using direct acid extraction and further propionylated and digested using trypsin to enable better separation on the mass spectrometer. Finally, samples were measured using LC-MS/MS; raw MS/MS data is shared on ProteomeXchange. The experimental spectra were identified using Mascot (Matrix Science) and further processed in Progenesis QIP (Nonlinear Dynamics, Waters). Due to the combinatorial explosion of hPTMs, a maximum set of 9 variable PTMs were identified in Mascot, namely acetylation (Ac), butyrylation (Bu), formylation (Fo), trimethylation (Me3) and ubiquitination (Ub) on K; dimethylation (Me2) and methylation (Me) on K and R; deamidation (Deam) on N,Q, R and phosphorylation (Ph) on S and T. Propionylation on K and N-termini were defined as fixed modifications. Since formylations (Fo) are chemically induced during sample preparation by adding formic acid, we can consider this PTM as unmodified. The hPTM atlas is publicly shared as a Progenesis QIP project on ProteomeXchange (ID: PXD031500), which is editable and reusable. Importantly, a quality control (QC) sample was made by mixing equal amounts of each sample, which was used to align all LC-MS/MS runs in Progenesis and normalize the overall histone load in each sample. Normalization against all histones is crucial, since we aim to identify changes in hPTMs and not the expression of histones themselves.

The above mentioned hPTM atlas was used to search for correlations between hPTMs and drug responses. Briefly, normalized abundances of all peptides from histone H3 and histone H4 were exported from Progenesis for all runs (after outlier removal). Next, the average fold change relative to the QC sample was calculated for each peptidoform in each cell line. These fold changes were used to correlate with IC50 and AUC values for each drug. This correlation was calculated in GraphPad Prism by using Spearman correlation, which shows the relation between two continuous variables; the IC50 or AUC values and hPTM fold changes. As a second, complementary correlation method, principle component analysis (PCA) was performed using Progenesis QIP by plotting the normalized abundances of all peptides from H3 and H4. PCA is a statistical procedure to observe trends, clusters and outliers (85,86). Within this approach, only the three most resistant and three most sensitive T-ALL cell lines were included for each compound.

4. RESULTS

4.1. CELL VIABILITY DATA

To determine the IC50, 21 T-ALL cell lines were treated with an increasing dose of three HDACis, namely PAN, ROM and VOR and three DNMTis, namely AZA, DAC and GSK.

4.1.1. DNMTis

As shown in **figure 4.1**, with the exception of HPB-ALL, PEER and TALL-1, AZA demonstrated a significant antiproliferative effect with a maximal reduction of cell viability to 0% at 50µM after 96h incubation time. Unlike AZA, DAC showed a low efficacy, since it did not reduce the viability to 0% for 16 of the 21 T-ALL cell lines at the highest drug concentration. However, as shown in **table 4.1**, for the majority of the cell lines, DAC showed a higher potency, given that the IC50 values are lower. Unexpectedly, the viability of the 21 T-ALL cell lines treated with GSK and incubated for six days, did not reduce to 0% at any concentration. Moreover, at the highest concentration viability mainly fluctuated between 20-60%, which represents a relative low efficacy. Furthermore, five cell lines, namely LOUCY, ALL-SIL, TAL-1, KARPAS-45JC and JURKAT did not reach the IC50 value with the concentration range used. Therefore, estimated IC50 values were used and the five cell lines were classified as resistant.

As shown in **table 4.1,** the IC50 values are more similar between AZA and DAC, compared to GSK. For instance, LOUCY treated with AZA and DAC demonstrated a low IC50 value of 0,2499 µM and 0,01 µM, respectively. In contrast, treatment of LOUCY with GSK showed a high IC50, namely 10 µM. This is also observed in TALL-1 with IC50 values of 0,3839 µM for AZA and 0,01 µM for DAC, whereas the IC50 value for GSK is 10 µM. This also applies to PEER, P-12 ICHIKAWA, JURKAT, ALL-SIL and DND-41. On the other hand, KARPAS-45 showed a remarkable high IC50 value for AZA and DAC, namely 10,73 µM and 50 µM, respectively, while a low IC50 value of 0,5 µM is observed for GSK.

As shown in **figure 4.1**, for some drugs, not all T-ALL cell lines reached 0% cell viability, which in turn leads to biased IC50 values. Therefore, AUC values were calculated since they more accurately represent the dose-response. It is important to note that the AUC values are not directly proportional to the IC50 values. As shown in **table 4.1**, LOUCY, DND-41, KOPTK-1 and JURKAT cell lines treated with AZA showed a low AUC value fluctuating between 1,5 and 3,5, whereas HSB-2, HPB-ALL, PEER and KARPAS-45 treated with AZA demonstrated a high AUC value ranging from 7 to 17. For cell lines treated with DAC, KOPTK-1, MOLT-16, PER-117, P12-ICHIKAWA and PEER displayed a low AUC value with lowest value of 0,8901 and highest value of 6,082. In contrast, SUPT-11, MOLT-4, CCRF-CEM, KARPAS-45 (JC), HPB-ALL, CUTTL1 and KARPAS-45 showed a high AUC value reaching 37,7. AUC values of GSK were less fluctuating, ranging from approximately 1,8 to 8,8, with the lowest values for KE-37, KOPT-K1, MOLT-16, KARPAS-45 and CUTTL1 as shown in **table 4.1**. Contrarily, LOUCY, TALL-1, SUP-T11 AND PER-117 demonstrated relatively higher AUC values, namely around 8.

As shown in **table 4.1**, AZA and DAC showed similarities, namely low AUC levels in LOUCY, MOLT-16, KOPT-K1, P12 ICHIKAWA, ALL-SIL and high AUC levels in MOLT-4, SUP-T11, HPB-ALL and KARPAS-45. However, high AUC levels were observed in PEER and TALL-1 treated with AZA, while the same cell lines demonstrated low AUC values when treated with DAC. After GSK treatment, similar to AZA and DAC, KE-37, KOPT-K1 and MOLT-16 demonstrated low AUC levels and SUP-T11 a high AUC level. Similar to what was observed for the IC50, KARPAS-45 showed a high AUC level for AZA and DAC, while a low AUC value for GSK.

Table 4.1: IC50 (µM) and AUC values for 21 T-ALL cell lines following treatment with azacytidine (AZA), decitabine (DAC) and GSK3685032 (GSK). IC50 values marked in grey were not reliable, since the cell viability does not reach 0%. Therefore, estimated IC50 values were used.

	IC50			AUC		
Cell line	AZA	DAC	GSK	AZA	DAC	GSK
ALL-SIL	1,202	0,35	10	4,163	8,216	6,257
CCRF-CEM	2,532	16	5	6,581	24,37	5,149
CUTTL1	1,349	50	0,5	5,997	33,72	3,031
DND-41	1,275	0,5	5	3,176	12,87	5,64
HPB-ALL	2	50	5	12,57	29,58	4,773
HSB-2	2,94	0,25	0,5	12,38	13,28	3,432
JURKAT	0,8094	0,5442	10	3,532	14,92	6,424
KARPAS-45	10,73	50	0,5	17,2	37,7	3,014
KARPAS-45 (JC)	1,715	8	10	5,603	24,59	6,935
KE-37	0,777	0,08383	0,3445	4,229	12,09	1,81
KOPT-K1	0,3271	0,01	0,2007	3,209	0,8901	2,245
LOUCY	0,2499	0,01	10	1,521	8,074	8,252
MOLT-16	1,807	0,01502	0,937	4,321	1,159	2,979
MOLT-4	4	0,6698	5	8,227	18,85	5,493
P12-ICHIKAWA	0,7699	0,06336	5,436	4,024	4,727	6,039
PEER	0,5931	0,0365	4,68	15,6	6,082	5,73
PER-117	2	0,1	9,182	5,937	4,171	8,834
PF-382	2,694	0,25	5	6,341	13,62	5,485
RPMI-8402	5,475	0,2892	0,9254	6,78	15,96	4,172
SUP-T11	2,838	1,254	9,58	8,539	18,22	8,426
TALL-1	0,3839	0,01	10	7,374	9,037	8,269

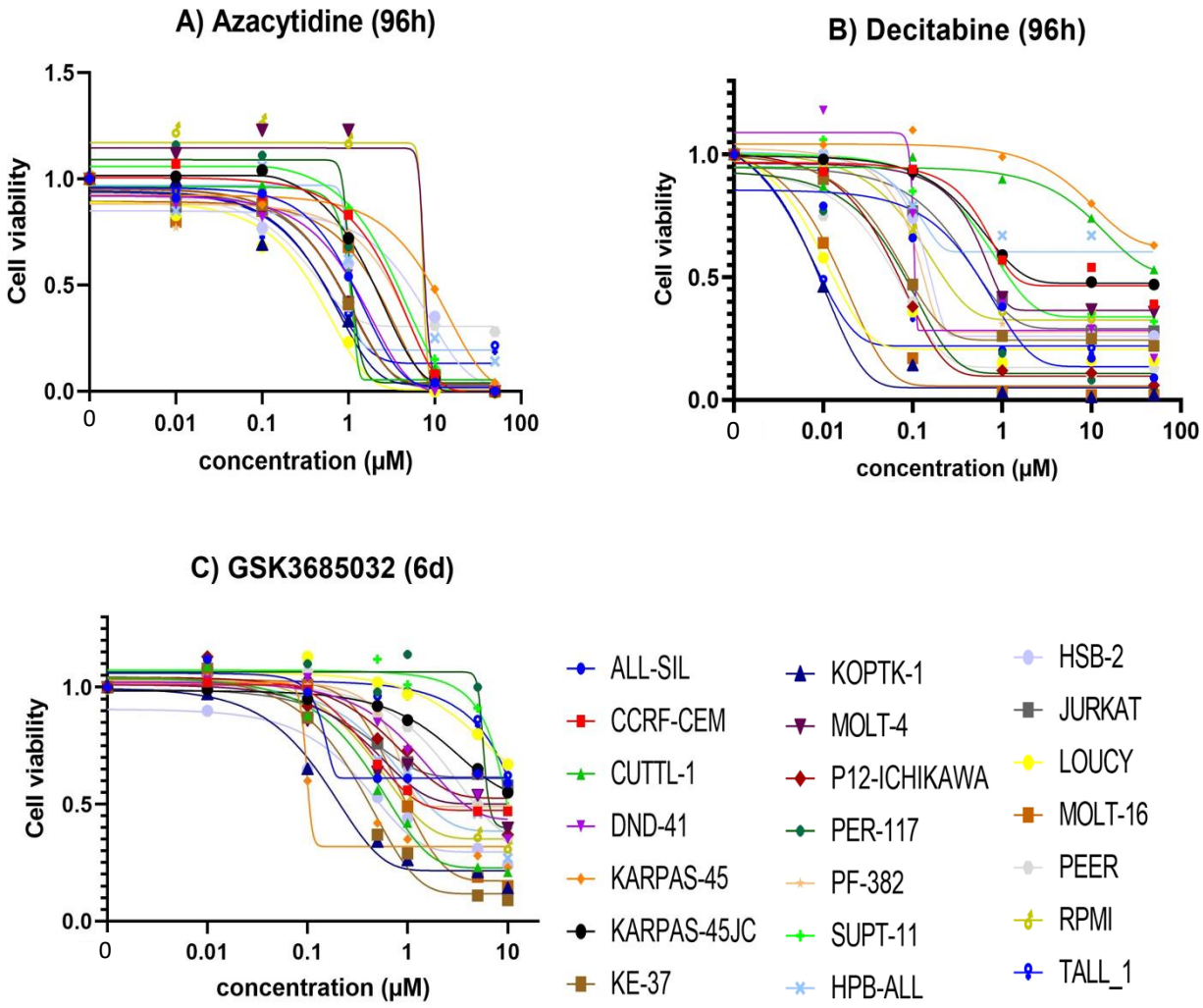

Figure 4.1: Survival curves showing cell viability of 21 T-ALL cell lines in response to a dilution series of A) azacytidine, B) decitabine, C) GSK3685032. Data points show the average of three independent experiments.

4.1.2. HDACis

As shown in **figure 4.2**, except for HPB-ALL and HSB-2, treating cell lines with ROM and VOR and incubating them for three days, reduced viability to 0% at the highest concentration 5 nM and 5 µM, respectively. For PAN, cell viability reduced to 0% for 18 of the 21 cell lines at the highest concentration (25 nM). As can be seen in **table 4.2**, the IC50 values of PAN and ROM were significantly lower in nanomolar range compared to VOR. Notably, for HPB-ALL, treatment with the six different epidrugs, never reduced cell viability to 0%, which emphasizes the resistance of HPB-ALL.

The IC50 values for ROM and VOR are less fluctuating, ranging from approximately 0,4 to 1,4, nanomolar for ROM and micromolar for VOR, while for PAN, they range from 5 nM up to 19 nM. JURKAT, KE-37, CCRF-CEM, MOLT-4, SUPT-11 and HPB-ALL overall have relatively high IC50 values for the three HDACis, while CUTTL-1, KARPAS-45, HSB-2, ALL-SIL and LOUCY demonstrated lower IC50 values. This indicates that there is less variation in sensitivity of the different cell lines to the three HDACis compared to the DNMTis.

Following VOR treatment, CUTTL1, RPMI-8402, LOUCY, PER-117 AND KOPT-K1 demonstrated low AUC values ranging from 0,5 to 0,8, whereas AUC values for JURKAT, SUP-T11 and KE-37 were about 2. As shown in **table 4.2**, cell lines treated with ROM gave a similar range of low AUCs, namely from approximately 0,6 to 0,8. Except for LOUCY, different cell lines are included in the lower AUC range of ROM compared to VOR, namely DND-41, MOLT-16, TALL-1 and PF-382. Higher AUC levels were found for ROM around 1,7 - 1,8, namely in SUP-T11, PER-117, RPMI-8402, JURKAT, KE-37, HSB-2 and HPB-ALL. In general, PAN showed higher AUC values, ranging from around 5 to 20, with KOPT-K1, KARPAS-45, CUTTL1 in the lower range and MOLT-4, KE-37, CCRF-CEM and JURKAT in the higher range. Noteworthy, the three HDACis all showed a high AUC level in JURKAT, HPB-ALL, KE-37, SUPT-11 cell lines, whereas low AUC levels were observed in LOUCY and CUTTL1.

Table 4.2: IC50 and AUC values for 21 T-ALL cell lines following treatment with azacytidine (AZA), decitabine (DAC) and GSK3685032. IC50 values marked in grey are not reliable, since the cell viability does not reach 0%.

	IC50			AUC		
Cell line	ROM (nM)	VOR (µM)	PAN (nM)	ROM	VOR	PAN
ALL-SIL	0,8554	0,6843	6,548	1,036	1,1	8,008
CCRF-CEM	1,202	0,9907	15,73	1,453	1,711	15,68
CUTTL1	0,7328	0,4418	5,629	0,8715	0,5003	6,61
DND-41	0,3704	0,7025	8,684	0,64	1,325	10,79
HPB-ALL	0,9949	0,8331	8,207	1,852	1,866	11,64
HSB-2	0,1021	0,5682	5,867	1,824	1,313	7,932
JURKAT	1,426	1,122	19,05	1,79	2,179	20,84
KARPAS-45	0,7937	0,6581	5,245	0,971	0,875	6,383
KARPAS-45 (JC)	1,188	0,6486	6,701	1,517	0,9078	8,517
KE-37	1,374	1,011	12,18	1,798	2,249	14,84
KOPT-K1	0,8788	0,5355	5,006	1,437	0,8013	5,348
LOUCY	0,6899	0,515	6,339	0,777	0,7748	7,766
MOLT-16	0,5735	0,73	8,161	0,652	1,299	11,42
MOLT-4	1,246	0,9358	9,836	1,564	1,656	12,21
P12-ICHIKAWA	1,226	0,7198	6,885	1,329	1,059	8,846
PEER	0,9	0,6367	7,48	1,129	0,9765	9,801
PER-117	1,422	0,5842	7,202	1,723	0,7938	9,045
PF-382	0,5823	0,6745	8,458	0,7639	1,17	11,67
RPMI-8402	1,179	0,5335	7,864	1,762	0,6133	9,878
SUP-T11	1,194	1,146	8,474	1,705	2,197	11,01
TALL-1	0,6695	0,6691	6,471	0,711	1,001	7,775

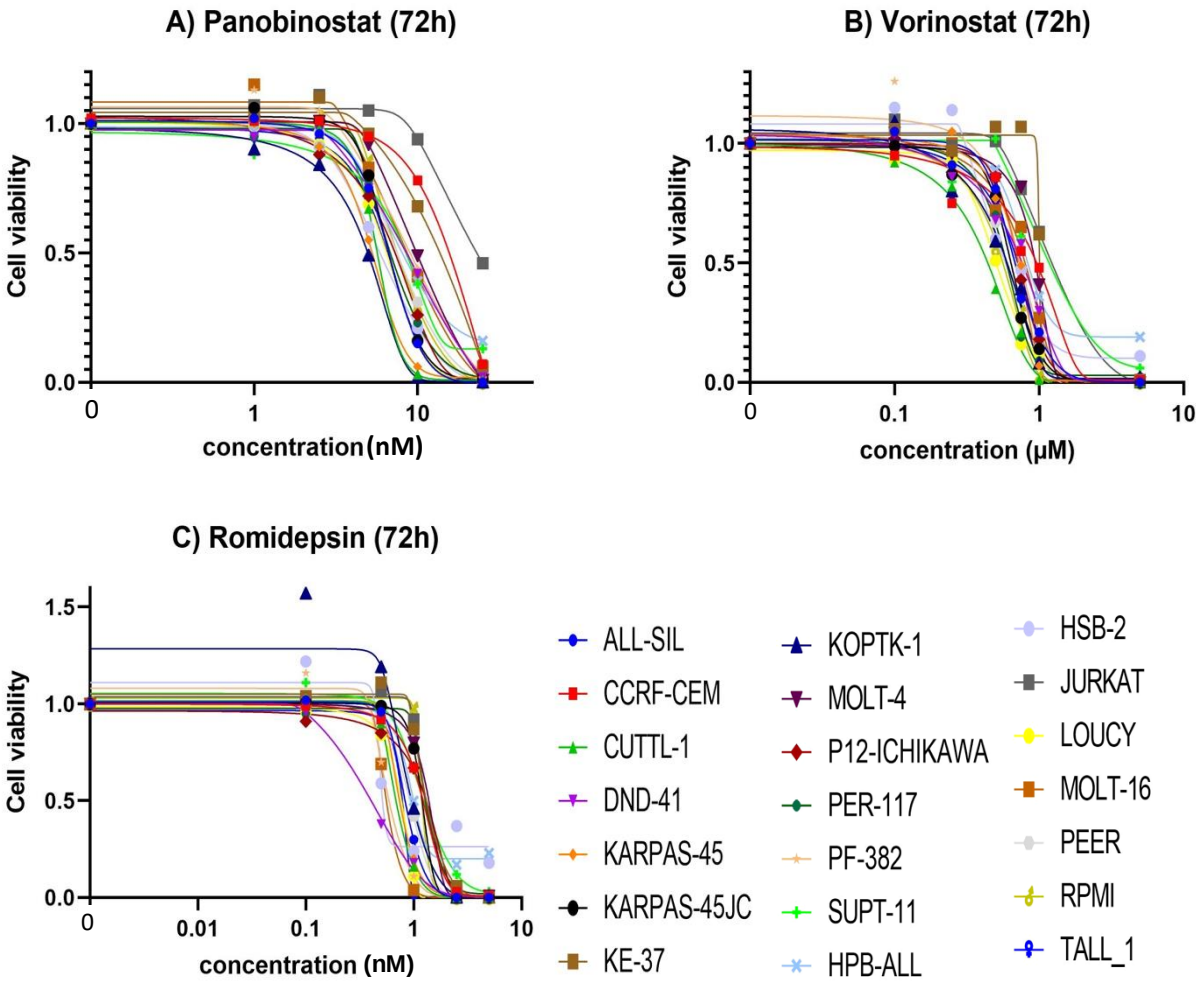

Figure 4.2: Survival curves showing cell viability of 21 T-ALL cell lines in response to a dilution series of A) panobinostat, B) vorinostat, and C) romidepsin. Data points show the average of three independent experiments.

4.2. hPTM CORRELATION

Baseline hPTM profiles of 21 T-ALL cell lines obtained by Provez et al. were used to search for correlations between hPTMs and drug response using two distinct methods. First, Spearman correlations were calculated including all cell lines and their corresponding AUC and IC50 values. Positive correlations (CF > 0) indicate a rise in the hPTM is correlated with a rise in IC50 and thus drug resistance. Likewise, negative correlations (CF < 0) indicate the hPTM is linked with sensitivity. Correlation factors lower than -0.5 or higher than 0.5 were considered significant. Secondly, PCA plots with the corresponding expression profiles showing the hPTM levels of the three most resistant and three most sensitive cell line were plotted for each drug.

4.2.1. DNMTis

As shown in **figure 4.3**, several positive correlations were found between IC50s and methylated peptides for the DNMTis. For example, between the peptidoform H4(4-17): K5[Fo] K8[Me2] and IC50 of cell lines treated with AZA, a Spearman correlation factor of 0,56 was found. Since we can consider lysins carrying formylations as unmodified, we can assume that an increase in H4 K8[Me2] increases the IC50 and thus resistance to AZA. This was also found for H4(4-17): K12[Me] K16[Ac], H4(20-35): K20[Me2], H3.1T(27-40): K37[Me2] R40[Me2] and H3.1T(27-40): K27[Me2] K37[Me2], with correlation factors of respectively 0,54, 0,5, 0,54 and 0,65.

Two of the peptidoforms mentioned above for AZA, positive correlations were demonstrated for DAC as well. This applies for H4(20-35): K20[Me2] and H3.1T(27-40): K37[Me2] R40[Me2], with a corresponding Spearman correlation factor of 0,50 and 0,51, respectively. Furthermore, significant Spearman correlation factors between other hPTMs and IC50 values of DAC in cell lines were observed, namely, H3.1T(9-17): K9[Me2], H3.1T(9-17): K9[Bu] and H3.3(18-26): K18[Bu], with correlation factors of respectively 0,62, 0,55 and 0,51. As regards GSK, no significant correlations were found between IC50 values and hPTMs. However, a Spearman correlation factor of 0,46 was found between H4(4-17): R17[Me] and IC50 values in cell lines treated with GSK.

For DAC, as illustrated in **figure 4.4**, Spearman correlation based on AUC levels showed equivalent results compared to correlations based on IC50 values for certain peptidoforms. For instance, H4(20-35): K20[Me2], H3.1T(9-17): K9[Me2], H3.3(18-26): K18[Bu] and H3.1T(27-40): K37[Me2] R40[Me2] showed a Spearman correlation of approximately 0,55 to 0,65, which further confirms that a rise in these hPTMs, suggests a rise in resistance to DAC. AZA showed a significant Spearman correlation factor of 0,55 between hPTM, namely H3.1T(9-17): K9[Me2] and AUC values of the cell lines treated with AZA. As was observed for Spearman correlation based on IC50 values, no significant correlation was found between hPTMs and AUC levels of cell lines treated with GSK, although H4(4-17): R17[Me] demonstrated a correlation factor of 0,46.

The hPTM profiles of the three most sensitive and three most resistant cell lines were investigated via PCA for each compound, which is shown in **Figure 4.5**. The expression profile of the most significant differential peptidoform between the two groups is displayed on the bottom of the corresponding PCA plot for each compound. For AZA, the most significant differential peptidoform between the sensitive and resistant group was H3(27-40): K27[Me2] K37[Me2], whereby a higher level is observed in the three most resistant cell lines, namely MOLT-4, RPMI-8402 and KARPAS-45. Contrarily, the three most sensitive cell lines, namely LOUCY, KOPT-K1 and TALL-1, showed relatively low levels of H3(27-40): K27[Me2] K37[Me2]. Furthermore, following the second most significant unmodified histone, H3(9-17): K9[Fo], the third most significant differential hPTM was H3(9-17): K9[Bu]. Interestingly, the three cell lines that were most sensitive to DAC, namely, LOUCY, KOPT-K1 and TALL-1, demonstrated significantly higher levels of H4(4-17): K8[Ac] K12[Ac] K16[Ac] compared to the three most resistant cell lines CUTTL1, HPB-ALL and KARPAS-45. Moreover, H4(4-17): K5[Ac] K12[Ac] K16[Ac] and H4(4-17): K12[Ac] K16[Ac] were the second and third most significant differential peptidoforms, respectively. Regarding GSK, the three most resistant cell lines, namely KARPAS-45JC, LOUCY and TALL-1, demonstrated significantly higher levels of H3(18-26): K18[Ac] K23[Ac] compared to the three most sensitive cell lines KOPT-K1, KE-37 and CUTTL1. The second and third most significant differential hPTMs were H3(27-40): K27[Bu] and H3(9-17): K9[Me3].

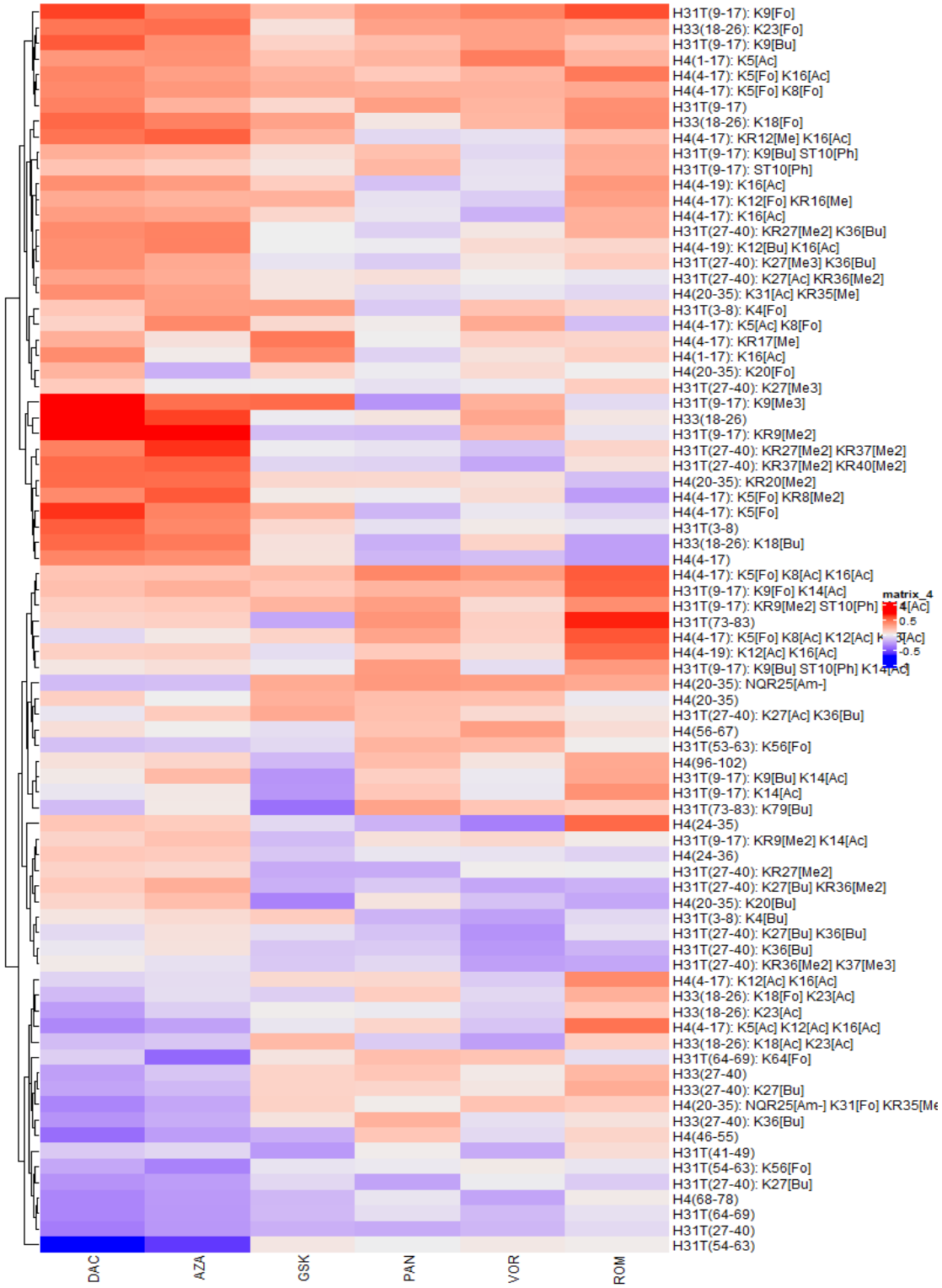

Figure 4.3: Heatmap of Spearman correlation factors between IC50 values and hPTMs for the six different drugs; azacytidine (AZA), decitabine (DAC), GSK3685032 (GSK), panobinostat (PAN), vorinostat (VOR) and romidepsin (ROM).

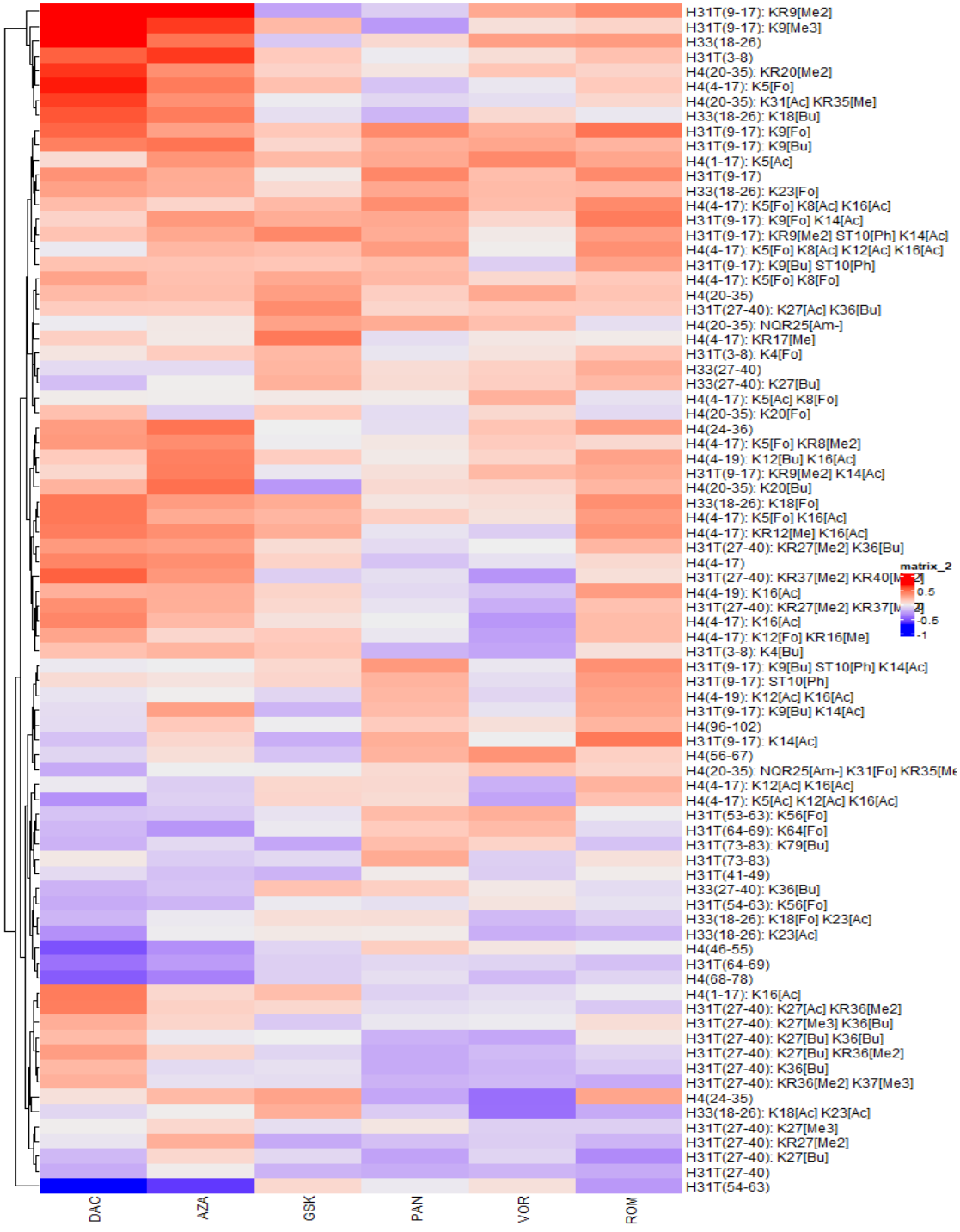

Figure 4.4: Heatmap of Spearman correlation factors between AUC values and hPTMs for the six different drugs; azacytidine (AZA), decitabine (DAC), GSK3685032 (GSK), panobinostat (PAN), vorinostat (VOR) and romidepsin (ROM).

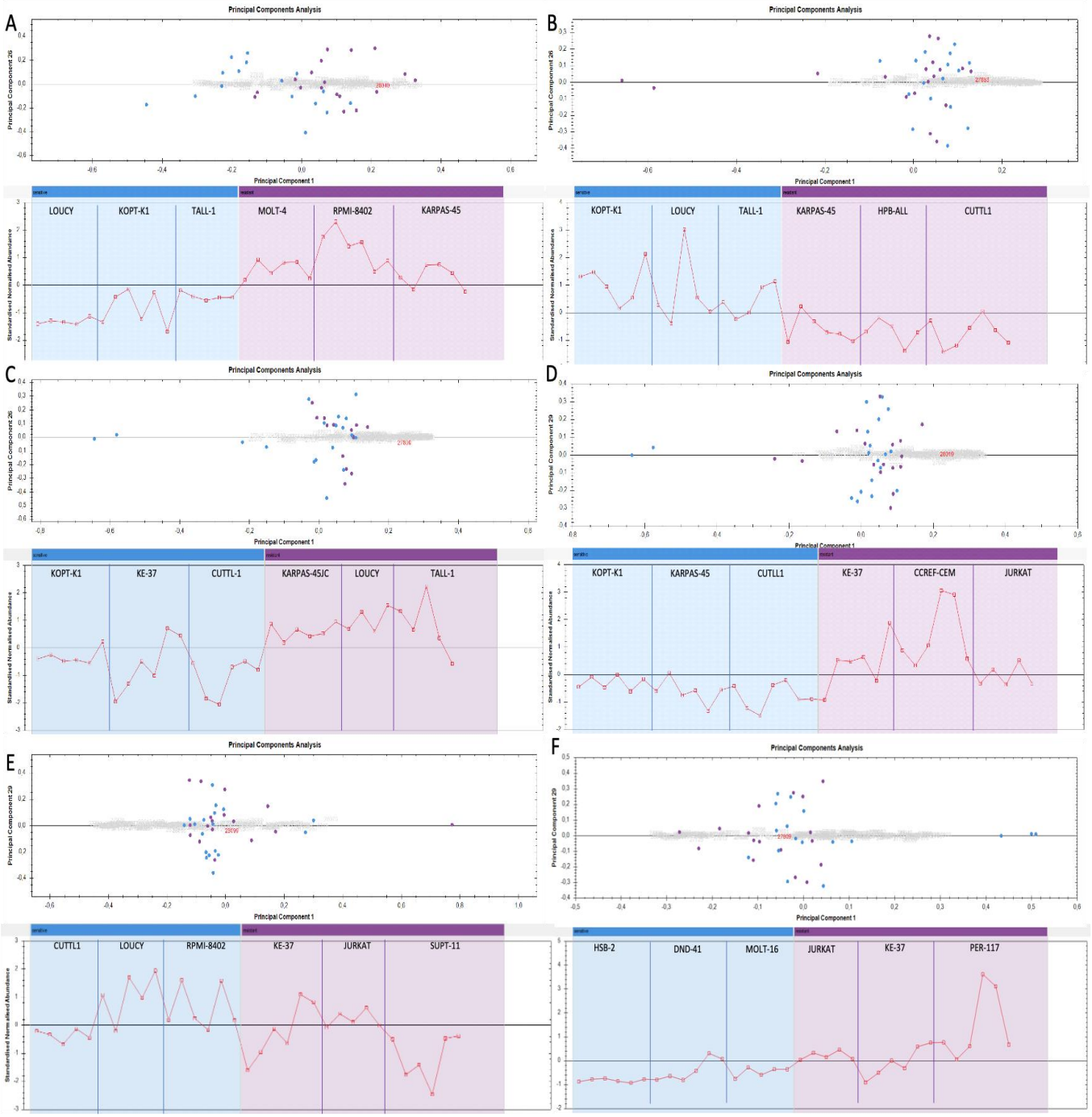

Figure 4.5: PCA plot of the normalized abundances of all peptides of H3 and H4 for the three most sensitive and three most resistant cell lines per drug. Sensitive cell lines are shown in blue, resistant cell lines in purple. Each dot represents one biological replicate. Furthermore, the expression profile of the most significant differential hPTM between the resistant and the sensitive group is shown per compound. A) AZA, B) DAC, C) GSK, D) PAN, E) VOR, F) ROM.

4.2.2. HDACis

As shown in **figure 4.3**, IC50 values of ROM demonstrated significant Spearman correlations of approximately 0,5 to 0,6 with the peptidoforms H4(4-17): K5[Fo] K8[Ac] K16[Ac], H4(4-17): K5[Fo] K8[Ac] K12[Ac] K16[Ac], H4(4-19): K12[Ac] K16[Ac] and H3.1T(9-17): K9[Fo] K14[Ac]. Therefore, an increase in these hPTMs is correlated with an increase in IC50, and thus resistance of the cell lines to ROM. However, for PAN and VOR, no significant Spearman correlation was found based on IC50, although some correlations are close to 0,5. For example a Spearman correlation factor of 0,41 between H4(4-17): K5[Fo] K8[Ac] K16[Ac] and IC50 values of PAN was found and a Spearman correlation of factor 0,44 was observed between H4(1-17): K5[Ac] and IC50 values in cell lines treated with VOR. Unfortunately, based on the AUC levels of the HDACis, no significant Spearman correlation was found.

As shown in **figure 4.5**, the three most sensitive cell lines for ROM, i.e. MOLT-16, HSB-2, DND-41 and two of the three most resistant cell lines, i.e. KE-37 and JURKAT, demonstrated similar low expression of H3(18-26): K18[Ac] K23[Ac]. However, PER-117, which is one of the three most resistant cell lines, showed distinctive higher levels of H3(18-26): K18[Ac] K23[Ac]. Furthermore, the second and third most significant differential hPTMs were H3(18-26): K18[Bu] and H3.3(27-40): K37[Bu]. For VOR, contrary to the sensitive cell line CUTTL1, peak levels of H3(18-26): K18[Ac] K23[Ac] were demonstrated in the other two of the three most sensitive cell lines, namely LOUCY and RPMI. Similar to the resistant JURKAT, low levels of H3(18-26): K18[Ac] K23[Ac] were seen in two of the three most sensitive cell lines, namely KE-37 and JURKAT. However, SUPT-11, which is one of the three most resistant cell line against VOR, showed a remarkable drop in H3(18-26): K18[Ac] K23[Ac] expression. As for PAN, the resistant CCRF-CEM showed remarkable higher levels of H3.3(27-40): K[Bu] compared to the three most sensitive cell lines, i.e. KOPT-K1, KARPAS-45, and CUTTL1. Likewise, the abundance of H3.3(27-40): K[Bu] was slightly higher for the other two resistant cell lines, namely KE-37 and JURKAT, compared to the three most sensitive cell lines treated with PAN (see figure 4.5, D).

5. DISCUSSION

5.1. CELL VIABILITY DATA

5.1.1. DNMTis

Cell viability of 21 human T-ALL cell lines treated with three different DNMTIs, namely AZA, DAC and GSK, was measured. As found in another study for AML (83), differences in potency and efficacy were observed between AZA and DAC, with AZA having a greater efficacy compared to DAC, since it reduced cell viability to 0% at the highest concentration for nearly all T-ALL cell lines. However, in general, DAC showed lower IC50 values indicating higher potency compared to AZA. This difference in potency and efficacy suggests that both drugs have different mode of action despite the fact that both drugs are classified as nucleoside based DNMTis. Both DNMTis incorporate into DNA, resulting in DNMT depletion and DNA hypomethylation. However, DAC only incorporates into DNA during the S-phase, whereas AZA also incorporates into RNA, which is possible in all cell phases and not restricted to the S-phase. According to Hollenbach et al, the plateau effect of DAC is caused by DNA incorporation restricted to the S-phase of cells, thereby affecting less cells. Therefore, prolonged treatment could further reduce cell viability (83,87).

Furthermore, as shown **in table 4.1**, AZA and DAC are more similar compared to GSK. For instance, the three most sensitive cell lines treated with AZA were equal to the three most sensitive DAC treated cell lines. Moreover, KARPAS-45 was the most resistant cell line for both AZA and DAC. As for GSK, contrasting results were observed. For instance, TALL-1 and LOUCY were the most resistant cell lines for GSK, while being most sensitive to AZA and DAC. This difference could be explained by the different mechanism of action of GSK as a non-nucleoside DNMTi. GSK did not reduce cell viability to 0% in any T-ALL cell line at the highest concentration. In addition, some cell lines treated with GSK, namely LOUCY, ALL-SIL, TAL-1, KARPAS-45JC and JURKAT, did not reach the IC50 value. Considering these observations, higher doses of GSK need to be tested. Interestingly, observing these differences, treatment stratification can be applied based on cell line. For instance, KARPAS-45 is sensitive to GSK, while resistant to DAC and AZA.

5.1.2. HDACis

HDACis are anticancer agents potentially restoring tumor suppressor genes, which showed promising results in lymphomas (88). Therefore, we measured the cell viability of 21 T-ALL cell lines treated with three HDACis, namely PAN, VOR and ROM. As shown in **figure 4.2**, the HDACis showed a high efficacy, whereby viability of at least 17 of the 21 cell lines was reduced to 0% at the highest concentration. Moreover, the ranking order of the sensitivity of the cell lines treated with the HDACis are more similar compared to cell lines treated with the DNMTis, which is observable in **table 4.2**. Given the similar degrees of sensitivity of the cell lines to the three HDACis, stratification of treatment only based on cell line is not applicable.

As shown in **figure 4.2**. In contrast to VOR, PAN and ROM, both showed effects and IC50 values at nanomolar range, which is also found in several other hematological and solid tumors (89–91). Noteworthy, PAN has a broader range of targets, inhibiting class I (HDACs 1, 2, 3, 8), II (HDACs 4, 5, 6, 7, 9, 10) and IV (HDAC 11) HDACs, while VOR only inhibit class I (HDAC 1, 2 and 3) and class II (HDAC 6). Similar to VOR, ROM only inhibits class I and II HDACs, in particular HDAC 1, 2, 4 and 6 (92–94). These remarkable differences in targets between the HDACis can potentially explain the different concentration ranges in effects and potency.

5.2. hPTM CORRELATION

Better stratification of T-ALL patients is needed, given that several problems occur during standard T-ALL treatment, including relapses, resistance and side effects. Since hPTMs have an important role in controlling gene expression, correlations between hPTMs and drug responses were investigated. Furthermore, hPTMs causing a significantly different drug response can potentially be used as biomarkers, which may contribute to personalized medicine.

5.2.1. DNMTis

As can be seen in **figure 4.3** and **figure 4.4**, several methylated peptides of H3 and H4 showed a significant positive correlation with the IC50 and AUC of the DNMTis AZA and DAC, and thus are linked with resistance. Since DNMTis cause hypomethylation of DNA, there could be a cross-talk between DNA methylation and histone methylation. Recently, this phenomenon was described by Li et al. They demonstrated that the protein UHRF1 recognizes hemi-methylated DNA and provides binding of DNMT1 to maintain DNA methylation. In addition, UHRF1 binds H3K9me3, which suggests an interplay between H3K9me3 and DNA methylation. Moreover, ubiquitin ligase activity of UHRF1 provides monoubiquitination of H3K18 and H3K23, whereby the ubiquitinated histones bind DNMT1 and further simulates DNMT1 methyltransferases activity. Furthermore, H3K36me3 interacts with DNMT3 causing H3K36me3-mediated DNA methylation (95–97). Given this cross play between DNA methylation and histone methylation, co-treatment with HMTis could be interesting.

For AZA, the expression profile of methylated histone peptides were higher in the three most resistant compared to the three most sensitive cell lines. This was further confirmed by the positive correlation between H3- and H4 methylation and IC50 of cell lines treated with AZA. As regards DAC, higher expression of acetylation was detected in the three most sensitive cell lines compared to the three most resistant cell lines, whereas for GSK, higher levels of histone acetylation were demonstrated in the three most resistant cell lines compared to the three most sensitive cell lines.

Given the high correlations between response to AZA and DAC and H3 and H4 methylation, these hPTMs could potentially be used as a predictive biomarkers for T-ALL treatment with AZA and DAC, whereby high H4 methylation is correlated with resistance and potentially therapy failure. To confirm these correlations, genes encoding the writers of these hPTMs can be knocked out or the writers themselves can be pharmacologically inhibited, i.e. by HMTis.

5.2.2. HDACis

ROM demonstrated several positive correlations between acetylated peptides of H3- and H4 and the IC50, which can be seen in **figure 4.3**. This suggests that Histone acetylation is correlated with resistance of the T-ALL cell lines against ROM. Noteworthy, in a study (98), high levels of H4 acetylation were demonstrated to be correlated with an increased overall survival. However, the authors reported that the study has to be confirmed, since limitations such as sample size and number of patients were present (98,99). Although H4 acetylation is correlated with resistance to ROM, it is important to note that H4 acetylation may be correlated with better prognosis, since it can restore repressed tumor suppressor genes. However, hyperacetylation in these cell lines can be explained by mutations in histone acetyltransferase (HAT), high expression of HAT and aberrant recruitment of HAT to wrong loci causing activation of oncogenes (100). Treating these cell lines with HDACi will not restore this alteration caused by aberrations in the HAT system.

Observing the expression profiles, relatively high abundance of histone acetylation was found in PER-117, which is one of the three most resistant cell lines against ROM. However, the other two resistant cell lines showed similar, but slightly higher acetylation degrees compared to the three most sensitive cell lines treated with ROM. These findings confirm the positive correlation between acetylation and IC50 values of ROM.

We demonstrated that ROM is positively correlated with H4 acetylation. However, further validation is needed by knocking out the genes encoding the writers of these hPTMs or by inhibiting the enzymes themselves.

6. CONCLUSION

AZA was found to be effective in reducing the cell viability of the T-ALL cell lines. However, the other two DNMTis, namely DAC and GSK demonstrated low efficacy. Although the higher efficacy of AZA compared to DAC, in general, lower IC50 values were demonstrated for DAC indicating higher potency of this epidrug. Further, IC50 values of AZA and DAC were more similar compared to GSK, whereby some cell lines were resistant against AZA and DAC, while sensitive to GSK. Conversely, other cell lines were sensitive against AZA and DAC, while resistant to GSK, which could be interesting for treatment stratification based on cell line. With regard to the HDACis, PAN, ROM and VOR, high efficacy was found, reducing the cell viability to approximately 0% in nearly all T-ALL cell lines. As for the IC50 values of the HDACis, PAN and ROM showed IC50 values at nanomolar range, while IC50 values of VOR were found to be in micromolar range.

Significant positive correlations were found between H3- and H4 methylation and IC50- and AUC values of the DNMTis, namely AZA and DAC. These correlations indicate that a high methylation level is linked with a high IC50 value, and thus resistance of the cell lines. Unfortunately, no significant correlations were found for GSK. As for the HDACis, IC50 values of ROM were positively correlated with H3- and H4 acetylation. This suggests that hyperacetylation is linked to resistance of the cell lines to ROM. No significant correlations were found between hPTMs and IC50 or AUC values of VOR and PAN.

Given the significant correlation between response to the epidrugs AZA, DAC and ROM, and the hPTM levels of the cell lines, it can be concluded that hPTMs could potentially be used as predictive biomarkers in T-ALL treatment. However, further validation is needed by knocking out the genes encoding the writers of these hPTMs or by pharmacologically inhibiting the writers themselves. If successful, this would enable stratification of T-ALL patients based on their hPTM signature to choose the best performing treatment.

7. REFERENCES

1. Annunziato AT. DNA Packaging: Nucleosomes and Chromatin. In: Nature Education. 2008.

2. Jeffries MA. The Development of Epigenetics in the Study of Disease Pathogenesis BT - Epigenetics in Allergy and Autoimmunity. In: Chang C, Lu Q, editors. Singapore: Springer Singapore; 2020. p. 57–94. Available from: https://doi.org/10.1007/978-981-15-3449-2_2

3. Agarwal SK, Weinstein LS. Chapter 2 - Epigenetics. In: Thakker R V, Whyte MP, Eisman JA, Igarashi TBT-G of BB and SD (Second E, editors. Academic Press; 2018. p. 25–32. Available from: https://www.sciencedirect.com/science/article/pii/B9780128041826000022

4. Zoya Marinova. Why ‘epidrugs’ will be the next major focus for precision medicine. Pharm J [Internet]. 2020; Available from: https://pharmaceutical-journal.com/article/opinion/why-epidrugs-will-be-the-next-major-focus-for-precision-medicine

5. Wilkinson J. Environmental Epigenetics: The Envirogenomic Interface. In: Dellasala DA, Goldstein MIBT-E of the A, editors. Oxford: Elsevier; 2018. p. 241–6. Available from: https://www.sciencedirect.com/science/article/pii/B9780128096659099110

6. Tamaru H. Confining euchromatin/heterochromatin territory: jumonji crosses the line. Genes Dev [Internet]. 2010 Jul 15;24(14):1465–78. Available from: https://pubmed.ncbi.nlm.nih.gov/20634313

7. What is Epigenetics | ZYMO RESEARCH [Internet]. [cited 2022 Feb 27]. Available from: https://www.zymoresearch.com/pages/what-is-epigenetics

8. Moore LD, Le T, Fan G. DNA Methylation and Its Basic Function. Neuropsychopharmacology [Internet]. 2013;38(1):23–38. Available from: https://doi.org/10.1038/npp.2012.112

9. Petryk N, Bultmann S, Bartke T, Defossez P-A. Staying true to yourself: mechanisms of DNA methylation maintenance in mammals. Nucleic Acids Res [Internet]. 2021 Apr 6;49(6):3020–32. Available from: https://doi.org/10.1093/nar/gkaa1154

10. Panni S, Lovering RC, Porras P, Orchard S. Non-coding RNA regulatory networks. Biochim Biophys Acta - Gene Regul Mech [Internet]. 2020;1863(6):194417. Available from: https://www.sciencedirect.com/science/article/pii/S1874939919302160

11. Bhan A, Soleimani M, Mandal SS. Long Noncoding RNA and Cancer: A New Paradigm. Cancer Res [Internet]. 2017 Aug 1;77(15):3965–81. Available from: https://doi.org/10.1158/0008-5472.CAN-16-2634

12. Biterge B, Schneider R. Histone variants: key players of chromatin. Cell Tissue Res [Internet]. 2014;356(3):457–66. Available from: https://doi.org/10.1007/s00441-014-1862-4

13. Talbert PB, Henikoff S. Histone variants at a glance. J Cell Sci [Internet]. 2021 Mar 26;134(6):jcs244749. Available from: https://pubmed.ncbi.nlm.nih.gov/33771851

14. Esteves de Lima J, Relaix F. Epigenetic Regulation of Myogenesis: Focus on the Histone Variants. Vol. 22, International Journal of Molecular Sciences . 2021.

15. Ramazi S, Zahiri J. Post-translational modifications in proteins: resources, tools and prediction methods. Database [Internet]. 2021 Oct 1;2021:baab012. Available from: https://doi.org/10.1093/database/baab012

16. Alquezar C, Arya S, Kao AW. Tau Post-translational Modifications: Dynamic Transformers of Tau Function, Degradation, and Aggregation [Internet]. Vol. 11, Frontiers in Neurology . 2021. Available from: https://www.frontiersin.org/article/10.3389/fneur.2020.595532

17. El Kennani S, Crespo M, Govin J, Pflieger D. Proteomic Analysis of Histone

Variants and Their PTMs: Strategies and Pitfalls. Vol. 6, Proteomes . 2018.

18. Audia JE, Campbell RM. Histone Modifications and Cancer. Cold Spring Harb Perspect Biol [Internet]. 2016 Apr 1;8(4):a019521–a019521. Available from: https://pubmed.ncbi.nlm.nih.gov/27037415

19. Liu Y. A peptidoform based proteomic strategy for studying functions of post-translational modifications. Proteomics [Internet]. 2022 Feb 1;22(4):2100316. Available from: https://doi.org/10.1002/pmic.202100316

20. Cheng Y, He C, Wang M, Ma X, Mo F, Yang S, et al. Targeting epigenetic regulators for cancer therapy: mechanisms and advances in clinical trials. Signal Transduct Target Ther [Internet]. 2019;4(1):62. Available from: https://doi.org/10.1038/s41392-019-0095-0

21. Bannister AJ, Kouzarides T. Regulation of chromatin by histone modifications. Cell Res [Internet]. 2011;21(3):381–95. Available from: https://doi.org/10.1038/cr.2011.22

22. Alaskhar Alhamwe B, Khalaila R, Wolf J, von Bülow V, Harb H, Alhamdan F, et al. Histone modifications and their role in epigenetics of atopy and allergic diseases. Allergy, Asthma Clin Immunol [Internet]. 2018;14(1):39. Available from: https://doi.org/10.1186/s13223-018-0259-4

23. Gujral P, Mahajan V, Lissaman AC, Ponnampalam AP. Histone acetylation and the role of histone deacetylases in normal cyclic endometrium. Reprod Biol Endocrinol [Internet]. 2020;18(1):84. Available from: https://doi.org/10.1186/s12958-020-00637-5

24. Dunphy K, Dowling P, Bazou D, O'Gorman P. Current Methods of Post-Translational Modification Analysis and Their Applications in Blood Cancers. Vol. 13, Cancers . 2021.

25. Soldi M, Cuomo A, Bremang M, Bonaldi T. Mass spectrometry-based proteomics

for the analysis of chromatin structure and dynamics. Int J Mol Sci [Internet]. 2013 Mar 6;14(3):5402–31. Available from: https://pubmed.ncbi.nlm.nih.gov/23466885

26. Wingren C. Antibody-Based Proteomics BT - Proteogenomics. In: Végvári Á, editor. Cham: Springer International Publishing; 2016. p. 163–79. Available from: https://doi.org/10.1007/978-3-319-42316-6_11

27. Sidoli S, Cheng L, Jensen ON. Proteomics in chromatin biology and epigenetics: Elucidation of post-translational modifications of histone proteins by mass spectrometry. J Proteomics [Internet]. 2012;75(12):3419–33. Available from: https://www.sciencedirect.com/science/article/pii/S187439191100710X

28. Shen T-L, Noon KR. Liquid Chromatography-Mass Spectrometry and Tandem Mass Spectrometry of Peptides and Proteins BT - HPLC of Peptides and Proteins: Methods and Protocols. In: Aguilar M-I, editor. Totowa, NJ: Springer New York; 2004. p. 111–39. Available from: https://doi.org/10.1385/1-59259-742-4:111

29. Liquid Chromatography [Internet]. Available from: https://chem.libretexts.org/@go/page/309

30. Banerjee S, Mazumdar S. Electrospray Ionization Mass Spectrometry: A Technique to Access the Information beyond the Molecular Weight of the Analyte. Wood TD, editor. Int J Anal Chem [Internet]. 2012;2012:282574. Available from: https://doi.org/10.1155/2012/282574

31. Saraswathy N, Ramalingam P. 12 - Mass spectrometry for proteomics. In: Saraswathy N, Ramalingam PBT-C and T in G and P, editors. Woodhead Publishing Series in Biomedicine [Internet]. Woodhead Publishing; 2011. p. 171–83. Available from: https://www.sciencedirect.com/science/article/pii/B9781907568107500122

32. Crotti S, Seraglia R, Traldi P. Some Thoughts on Electrospray Ionization Mechanisms. Eur J Mass Spectrom [Internet]. 2011 Apr 1;17(2):85–99. Available from: https://doi.org/10.1255/ejms.1129

33. Allen DR, McWhinney BC. Quadrupole Time-of-Flight Mass Spectrometry: A Paradigm Shift in Toxicology Screening Applications. Clin Biochem Rev [Internet]. 2019 Aug;40(3):135–46. Available from: https://pubmed.ncbi.nlm.nih.gov/31530964

34. March RE. Quadrupole ion traps. Mass Spectrom Rev [Internet]. 2009 Nov 1;28(6):961–89. Available from: https://doi.org/10.1002/mas.20250

35. David W. Koppenaal, Charles J. Barinaga, M. Bonner Denton, Roger P. Sperline, Gary M. Hieftje, Gregory D. Schilling, et al. MS Detectors [Internet]. 2005 [cited 2022 Mar 9]. p. 419–27. Available from: https://pubs.acs.org/doi/pdf/10.1021/ac053495p

36. Wiza JL. MICROCHANNEL PLATE DETECTORS. Nucl Instruments Methods. 1979;162:587–601.

37. Cai H, Sun Y, Zhang X, Zhang L, Liu H, Li Q, et al. Reduction Temperature-Dependent Nanoscale Morphological Transformation and Electrical Conductivity of Silicate Glass Microchannel Plate. Vol. 12, Materials . 2019.

38. Britton L-MP, Gonzales-Cope M, Zee BM, Garcia BA. Breaking the histone code with quantitative mass spectrometry. Expert Rev Proteomics [Internet]. 2011 Oct;8(5):631–43. Available from: https://pubmed.ncbi.nlm.nih.gov/21999833

39. Quantitative Proteomics [Internet]. [cited 2022 Mar 9]. Available from: https://www.helmholtz-munich.de/proteomics/research/technology/quantitative-proteomics/label-free-dda-dia/index.html

40. Ten-Doménech I, Martínez-Sena T, Moreno-Torres M, Sanjuan-Herráez JD, Castell J V, Parra-Llorca A, et al. Comparing Targeted vs. Untargeted MS(2) Data-Dependent Acquisition for Peak Annotation in LC-MS Metabolomics. Metabolites [Internet]. 2020 Mar 26;10(4):126. Available from: https://pubmed.ncbi.nlm.nih.gov/32225041

41. Data-dependent versus data-independent acquisition [Internet]. [cited 2022 Mar

16]. Available from: http://ajscientific.blogspot.com/2018/04/data-dependent-versus-data-independent.html

42. Marquioni V, Nunes FMF, Novo-Mansur MTM. Protein Identification by Database Searching of Mass Spectrometry Data in the Teaching of Proteomics. J Chem Educ [Internet]. 2021 Mar 9;98(3):812–23. Available from: https://doi.org/10.1021/acs.jchemed.0c00853

43. Anand S, Samuel M, Ang C-S, Keerthikumar S, Mathivanan S. Label-Based and Label-Free Strategies for Protein Quantitation BT - Proteome Bioinformatics. In: Keerthikumar S, Mathivanan S, editors. New York, NY: Springer New York; 2017. p. 31–43. Available from: https://doi.org/10.1007/978-1-4939-6740-7_4

44. Megger DA, Bracht T, Meyer HE, Sitek B. Label-free quantification in clinical proteomics. Biochim Biophys Acta - Proteins Proteomics [Internet]. 2013;1834(8):1581–90. Available from: https://www.sciencedirect.com/science/article/pii/S1570963913001556

45. Perkins DN, Pappin DJC, Creasy DM, Cottrell JS. Probability-based protein identification by searching sequence databases using mass spectrometry data. Electrophoresis [Internet]. 1999 Dec 1;20(18):3551–67. Available from: https://doi.org/10.1002/(SICI)1522-2683(19991201)20:18%3C3551::AID-ELPS3551%3E3.0.CO

46. Berdasco M, Esteller M. Aberrant Epigenetic Landscape in Cancer: How Cellular Identity Goes Awry. Dev Cell [Internet]. 2010 Nov 16;19(5):698–711. Available from: https://doi.org/10.1016/j.devcel.2010.10.005

47. Lu Y, Chan Y-T, Tan H-Y, Li S, Wang N, Feng Y. Epigenetic regulation in human cancer: the potential role of epi-drug in cancer therapy. Mol Cancer [Internet]. 2020;19(1):79. Available from: https://doi.org/10.1186/s12943-020-01197-3

48. Chen JF, Yan Q. The roles of epigenetics in cancer progression and metastasis. Biochem J [Internet]. 2021 Sep 14;478(17):3373–93. Available from:

https://doi.org/10.1042/BCJ20210084

49. Piunti A, Shilatifard A. The roles of Polycomb repressive complexes in mammalian development and cancer. Nat Rev Mol Cell Biol [Internet]. 2021;22(5):326–45. Available from: https://doi.org/10.1038/s41580-021-00341-1

50. Bonner WM, Redon CE, Dickey JS, Nakamura AJ, Sedelnikova OA, Solier S, et al. GammaH2AX and cancer. Nat Rev Cancer [Internet]. 2008/11/13. 2008 Dec;8(12):957–67. Available from: https://pubmed.ncbi.nlm.nih.gov/19005492

51. Miranda Furtado CL, Dos Santos Luciano MC, Silva Santos R Da, Furtado GP, Moraes MO, Pessoa C. Epidrugs: targeting epigenetic marks in cancer treatment. Epigenetics [Internet]. 2019/07/13. 2019 Dec;14(12):1164–76. Available from: https://pubmed.ncbi.nlm.nih.gov/31282279

52. Sharma S, Kelly TK, Jones PA. Epigenetics in cancer. Carcinogenesis [Internet]. 2009/09/13. 2010 Jan;31(1):27–36. Available from: https://pubmed.ncbi.nlm.nih.gov/19752007

53. Baylin SB, Jones PA. Epigenetic Determinants of Cancer. Cold Spring Harb Perspect Biol [Internet]. 2016 Sep 1;8(9):a019505. Available from: https://pubmed.ncbi.nlm.nih.gov/27194046

54. Girardi T, Vicente C, Cools J, De Keersmaecker K. The genetics and molecular biology of T-ALL. Blood [Internet]. 2017 Mar 2;129(9):1113–23. Available from: https://doi.org/10.1182/blood-2016-10-706465

55. Peirs S, Van Der Meulen J, Taghon T, Speleman F, Poppe B, Van Vlierberghe P, et al. Epigenetics in T-cell acute lymphoblastic leukemia. 2014.

56. Definition of immunophenotyping - NCI Dictionary of Cancer Terms - NCI [Internet]. [cited 2022 May 8]. Available from: https://www.cancer.gov/publications/dictionaries/cancer-terms/def/immunophenotyping

57. Van der Meulen J, Van Roy N, Van Vlierberghe P, Speleman F. The epigenetic landscape of T-cell acute lymphoblastic leukemia. Int J Biochem Cell Biol [Internet]. 2014;53:547–57. Available from: https://www.sciencedirect.com/science/article/pii/S1357272514001307

58. Montalvo-Casimiro M, González-Barrios R, Meraz-Rodriguez MA, Juárez-González VT, Arriaga-Canon C, Herrera LA. Epidrug Repurposing: Discovering New Faces of Old Acquaintances in Cancer Therapy [Internet]. Vol. 10, Frontiers in Oncology . 2020. Available from: https://www.frontiersin.org/article/10.3389/fonc.2020.605386

59. Citron F, Fabris L. Targeting Epigenetic Dependencies in Solid Tumors: Evolutionary Landscape Beyond Germ Layers Origin. Vol. 12, Cancers . 2020.

60. Wong KK. DNMT1: A key drug target in triple-negative breast cancer. Semin Cancer Biol [Internet]. 2021;72:198–213. Available from: https://www.sciencedirect.com/science/article/pii/S1044579X20301097

61. Huang S, Stillson NJ, Sandoval JE, Yung C, Reich NO. A novel class of selective non-nucleoside inhibitors of human DNA methyltransferase 3A. Bioorg Med Chem Lett [Internet]. 2021;40:127908. Available from: https://www.sciencedirect.com/science/article/pii/S0960894X21001347

62. Hu C, Liu X, Zeng Y, Liu J, Wu F. DNA methyltransferase inhibitors combination therapy for the treatment of solid tumor: mechanism and clinical application. Clin Epigenetics [Internet]. 2021;13(1):166. Available from: https://doi.org/10.1186/s13148-021-01154-x

63. Mehdipour P, Chen R, De Carvalho DD. The next generation of DNMT inhibitors. Nat Cancer [Internet]. 2021;2(10):1000–1. Available from: https://doi.org/10.1038/s43018-021-00271-z

64. Ganesan A, Arimondo PB, Rots MG, Jeronimo C, Berdasco M. The timeline of epigenetic drug discovery: from reality to dreams. Clin Epigenetics [Internet]. 2019;11(1):174. Available from: https://doi.org/10.1186/s13148-019-0776-0

65. Pappalardi MB, Keenan K, Cockerill M, Kellner WA, Stowell A, Sherk C, et al. Discovery of a first-in-class reversible DNMT1-selective inhibitor with improved tolerability and efficacy in acute myeloid leukemia. Nat Cancer [Internet]. 2021;2(10):1002–17. Available from: https://doi.org/10.1038/s43018-021-00249-x

66. Yang T, Yang Y, Wang Y. Predictive biomarkers and potential drug combinations of epi-drugs in cancer therapy. Clin Epigenetics [Internet]. 2021;13(1):113. Available from: https://doi.org/10.1186/s13148-021-01098-2

67. Losson H, Schnekenburger M, Dicato M, Diederich M. Natural Compound Histone Deacetylase Inhibitors (HDACi): Synergy with Inflammatory Signaling Pathway Modulators and Clinical Applications in Cancer. Molecules [Internet]. 2016 Nov 23;21(11):1608. Available from: https://pubmed.ncbi.nlm.nih.gov/27886118

68. azacitidine [Internet]. [cited 2022 Apr 20]. Available from: https://www.farmacotherapeutischkompas.nl/bladeren/preparaatteksten/a/azacitidine#indicaties

69. panobinostat [Internet]. [cited 2022 Apr 20]. Available from: https://www.farmacotherapeutischkompas.nl/bladeren/preparaatteksten/p/panobinostat#indicaties

70. decitabine [Internet]. [cited 2022 Apr 20]. Available from: https://www.farmacotherapeutischkompas.nl/bladeren/preparaatteksten/d/decitabine#indicaties

71. Volker M. Lauschke IB and MI-S. Pharmacoepigenetics and Toxicoepigenetics: Novel Mechanistic Insights and Therapeutic Opportunities. Annu Rev [Internet]. 2017;58:161-185. Available from: https://www.annualreviews.org/doi/full/10.1146/annurev-pharmtox-010617-053021#_i24

72. Abdullah-Koolmees H, van Keulen AM, Nijenhuis M, Deneer VHM. Pharmacogenetics Guidelines: Overview and Comparison of the DPWG, CPIC,

CPNDS, and RNPGx Guidelines. Front Pharmacol [Internet]. 2021 Jan 25;11:595219. Available from: https://pubmed.ncbi.nlm.nih.gov/33568995

73. Majchrzak-Celińska A, Baer-Dubowska W. Chapter 2 - Pharmacoepigenetics: Basic Principles for Personalized Medicine. In: Cacabelos RBT-P, editor. Translational Epigenetics [Internet]. Academic Press; 2019. p. 101–12. Available from: https://www.sciencedirect.com/science/article/pii/B9780128139394000024

74. Cacabelos R, Carril JC, Sanmartín A, Cacabelos P. Chapter 6 - Pharmacoepigenetic Processors: Epigenetic Drugs, Drug Resistance, Toxicoepigenetics, and Nutriepigenetics. In: Cacabelos RBT-P, editor. Translational Epigenetics [Internet]. Academic Press; 2019. p. 191–424. Available from: https://www.sciencedirect.com/science/article/pii/B9780128139394000061

75. Teijido O. Chapter 3 - Epigenetic Mechanisms in the Regulation of Drug Metabolism and Transport. In: Cacabelos RBT-P, editor. Translational Epigenetics [Internet]. Academic Press; 2019. p. 113–28. Available from: https://www.sciencedirect.com/science/article/pii/B9780128139394000036

76. Aberuyi N, Rahgozar S, Ghodousi ES, Ghaedi K. Drug Resistance Biomarkers and Their Clinical Applications in Childhood Acute Lymphoblastic Leukemia. Front Oncol [Internet]. 2020 Jan 17;9:1496. Available from: https://pubmed.ncbi.nlm.nih.gov/32010613

77. Roman-Gomez J, Jimenez-Velasco A, Agirre X, Prosper F, Heiniger A, Torres A. Lack of CpG Island Methylator Phenotype Defines a Clinical Subtype of T-Cell Acute Lymphoblastic Leukemia Associated With Good Prognosis. J Clin Oncol [Internet]. 2005 Oct 1;23(28):7043–9. Available from: https://doi.org/10.1200/JCO.2005.01.4944

78. Roman-Gomez J, Jimenez-Velasco A, Castillejo JA, Agirre X, Barrios M, Navarro G, et al. Promoter hypermethylation of cancer-related genes: a strong independent prognostic factor in acute lymphoblastic leukemia. Blood [Internet].

2004;104(8):2492–8. Available from: https://www.sciencedirect.com/science/article/pii/S0006497120433130

79. Moreno DA, Scrideli CA, Cortez MAA, De Paula Queiroz R, Valera ET, Da Silva Silveira V, et al. research paper: Differential expression of HDAC3, HDAC7 and HDAC9 is associated with prognosis and survival in childhood acute lymphoblastic leukaemia. Br J Haematol [Internet]. 2010 Sep 1;150(6):665–73. Available from: https://doi.org/10.1111/j.1365-2141.2010.08301.x

80. Maćkowska N, Drobna-Śledzińska M, Witt M, Dawidowska M. DNA Methylation in T-Cell Acute Lymphoblastic Leukemia: In Search for Clinical and Biological Meaning. Int J Mol Sci [Internet]. 2021 Jan 30;22(3):1388. Available from: https://pubmed.ncbi.nlm.nih.gov/33573325

81. Cordo' V, van der Zwet JCG, Canté-Barrett K, Pieters R, Meijerink JPP. T-cell Acute Lymphoblastic Leukemia: A Roadmap to Targeted Therapies. Blood Cancer Discov [Internet]. 2021 Jan 13;2(1):19–31. Available from: https://doi.org/10.1158/2643-3230.BCD-20-0093

82. German Collection of Microorganisms and Cell Cultures GmbH: Welcome to the Leibniz Institute DSMZ [Internet]. [cited 2022 May 6]. Available from: https://www.dsmz.de/

83. Hollenbach PW, Nguyen AN, Brady H, Williams M, Ning Y, Richard N, et al. A comparison of azacitidine and decitabine activities in acute myeloid leukemia cell lines. PLoS One [Internet]. 2010 Feb 2;5(2):e9001–e9001. Available from: https://pubmed.ncbi.nlm.nih.gov/20126405

84. Provez L, Van Puyvelde B, Corveleyn L, Demeulemeester N, Verhelst S, Lintermans B, et al. Title An interactive mass spectrometry atlas of histone posttranslational modifications in T-cell acute leukemia. [cited 2022 May 31]; Available from: https://doi.org/10.1101/2022.05.05.490796

85. What Is Principal Component Analysis (PCA) and How It Is Used? [Internet]. [cited

2022 May 22]. Available from: https://www.sartorius.com/en/knowledge/science-snippets/what-is-principal-component-analysis-pca-and-how-it-is-used-507186

86. Correlation Coefficient: Simple Definition, Formula, Easy Calculation Steps [Internet]. [cited 2022 May 22]. Available from: https://www.statisticshowto.com/probability-and-statistics/correlation-coefficient-formula/

87. Derissen EJB, Beijnen JH, Schellens JHM. Concise drug review: azacitidine and decitabine. Oncologist [Internet]. 2013/05/13. 2013;18(5):619–24. Available from: https://pubmed.ncbi.nlm.nih.gov/23671007

88. Chen I-C, Sethy B, Liou J-P. Recent Update of HDAC Inhibitors in Lymphoma [Internet]. Vol. 8, Frontiers in Cell and Developmental Biology . 2020. Available from: https://www.frontiersin.org/article/10.3389/fcell.2020.576391

89. Dias JNR, Aguiar SI, Pereira DM, André AS, Gano L, Correia JDG, et al. The histone deacetylase inhibitor panobinostat is a potent antitumor agent in canine diffuse large B-cell lymphoma. Oncotarget; Vol 9, No 47 [Internet]. 2018; Available from: https://www.oncotarget.com/article/25580/text/

90. Cosenza M, Civallero M, Fiorcari S, Pozzi S, Marcheselli L, Bari A, et al. The histone deacetylase inhibitor romidepsin synergizes with lenalidomide and enhances tumor cell death in T-cell lymphoma cell lines. Cancer Biol Ther [Internet]. 2016/09/22. 2016 Oct 2;17(10):1094–106. Available from: https://pubmed.ncbi.nlm.nih.gov/27657380

91. Bernhart E, Stuendl N, Kaltenegger H, Windpassinger C, Donohue N, Leithner A, et al. Histone deacetylase inhibitors vorinostat and panobinostat induce G1 cell cycle arrest and apoptosis in multidrug resistant sarcoma cell lines. Oncotarget [Internet]. 2017 Aug 24;8(44):77254–67. Available from: https://pubmed.ncbi.nlm.nih.gov/29100385

92. Romidepsin: Uses, Interactions, Mechanism of Action | DrugBank Online [Internet].

[cited 2022 May 29]. Available from: https://go.drugbank.com/drugs/DB06176

93. Panobinostat: Uses, Interactions, Mechanism of Action | DrugBank Online [Internet]. [cited 2022 May 29]. Available from: https://go.drugbank.com/drugs/DB06603

94. Vorinostat: Uses, Interactions, Mechanism of Action | DrugBank Online [Internet]. [cited 2022 May 29]. Available from: https://go.drugbank.com/drugs/DB02546

95. Li Y, Chen X, Lu C. The interplay between DNA and histone methylation: molecular mechanisms and disease implications. EMBO Rep [Internet]. 2021 May 5;22(5):e51803. Available from: https://doi.org/10.15252/embr.202051803

96. UHRF1 - E3 ubiquitin-protein ligase UHRF1 - Homo sapiens (Human) - UHRF1 gene & protein [Internet]. [cited 2022 May 29]. Available from: https://www.uniprot.org/uniprot/Q96T88

97. Kubota T. The Mechanisms of Epigenetic Modifications During DNA Replication. In: Miyake K, editor. Rijeka: IntechOpen; 2013. p. Ch. 13. Available from: https://doi.org/10.5772/51592

98. Advani AS, Gibson SE, Douglas E, Jin T, Zhao X, Kalaycio M, et al. Histone H4 acetylation by immunohistochemistry and prognosis in newly diagnosed adult acute lymphoblastic leukemia (ALL) patients. BMC Cancer [Internet]. 2010 Jul 21;10:387. Available from: https://pubmed.ncbi.nlm.nih.gov/20663136

99. Zhang C, Zhong JF, Stucky A, Chen X-L, Press MF, Zhang X. Histone acetylation: novel target for the treatment of acute lymphoblastic leukemia. Clin Epigenetics [Internet]. 2015 Nov 4;7:117. Available from: https://pubmed.ncbi.nlm.nih.gov/26543507

100. Di Cerbo V, Schneider R. Cancers with wrong HATs: the impact of acetylation. Brief Funct Genomics [Internet]. 2013 May 1;12(3):231–43. Available from: https://doi.org/10.1093/bfgp/els065

101. Human T-ALL Cell Lines – An informative database for human T-ALL cell lines. [Internet]. [cited 2022 Jun 5]. Available from: https://humantallcelllines.wordpress.com/

8. APPENDIX

Table 1: Epigenetic biomarkers, miRNAs, F = favorable, U = unfavorable (76)

miRNA	**Type of biomarker**	**prognosis**	**Lineage**
miRNAs			
miR-100, miR-99a	Downregulation	U	T
miR-335	Downregulation	U	B, T
miR-326	Downregulation	U	B, T
miR-335-3p	Downregulation	U	B, T
miR-7, miR-216, miR100	Upregulation	U	B, T
miR-486, miR-191, miR-150, miR-487, miR-342	Downregulation	U	B, T
miR-128b	Upregulation	F	B, T
miR-223	Downregulation	U	B, T
miR-24	Downregulation	U	B, T
miR-16	Downregulation	F	B, T
miR-33, miR-215, miR-369-5p, miR496, miR-518, miR-599	Upregulation	U	B, T
miR-10a, miR-134, miR-214, miR-484, miR-572, miR-580, miR-624, miR-627	Upregulation	F	B, T
miR-210	Downregulation	U	B, T
miR143, miR-182	Downregulation	U	B, T
miR-155a	Upregulation	U	B, T

Table 2: T-ALL cell lines used and their characteristics, WT: wildtype, MUT: mutated (101).

CELL LINE	ONCOGENE GROUP	*CDKN2A*	*CREBBP*	*FBXW7*	*HRAS*	*JAK1*	*KRAS*	*MYB*	*NOTCH1*	*NRAS*	*PTEN*	*TP53*
ALL-SIL	*TLX1*	MUT		WT		MUT		MUT	MUT		WT	
CCRF-CEM	*TAL1*	MUT		MUT			MUT	MUT	WT/MUT		MUT	MUT
CUTTL-1												
TALL-1				MUT					WT	MUT	WT	MUT
DND-41	*TLX3*	WT/MUT	MUT	WT		MUT	MUT		MUT	MUT	WT/MUT	MUT
HPB-ALL	*TLX3*	MUT	MUT	WT/MUT	MUT	MUT			MUT		WT/MUT	MUT
HSB-2	*TAL1*	MUT		MUT		MUT			WT/MUT	MUT	WT	WT
JURKAT	*TAL1*	MUT	MUT	MUT		MUT	WT	WT	WT/MUT		MUT	MUT
KARPAS-45		WT/MUT	MUT	MUT				MUT	MUT		MUT	MUT
CUTTL1												
KOPT-K1	*TAL1*	MUT	MUT	WT				WT/MUT	MUT		WT	MUT
LOUCY	*ETP*	MUT	WT	WT		MUT		WT/MUT	WT		MUT	MUT
MOLT-4	*TAL1*	MUT	MUT	WT	MUT	MUT		MUT	MUT	MUT	MUT	WT/MUT
MOLT-16	*TAL1*	MUT		WT		MUT		WT/MUT	WT		WT/MUT	WT/MUT
P12-ICHIKAWA	*LMO2*	MUT	WT	MUT		MUT	WT	MUT	MUT/WT	MUT	MUT	
PEER		MUT	WT	WT/MUT		MUT			WT/MUT		WT	MUT
PF-382	*TAL1*		MUT	WT	MUT	MUT		WT	MUT	MUT	MUT	MUT
RPMI-8402	*TAL1* *LMO1*	MUT	MUT	MUT	MUT	MUT		MUT	MUT /WT		MUT	WT/MUT
KE-37		MUT						MUT	WT/MUT		MUT	
SUP-T1			MUT	WT		MUT			WT		WT/MUT	MUT

Master dissertation submitted to the faculty of Pharmaceutical Sciences, performed in collaboration with the Laboratory of Pharmaceutical Biotechnology

Promotor: dr. Maarten Dhaenens

Commissioners: Prof. dr. Dieter Deforce and dr. Tim Pieters